

POLITECNICO DI TORINO

Department of Control and Computer Engineering

Master degree course in Mechatronic Engineering

Master Degree Thesis

**Development a bio-motioning
patch for continuous monitoring of
heart rate**



Supervisors

prof. Marcello Chiaberge

prof. Mahmoud Tavakoli

Candidate

Alessandro Marra

April 2018

Contents

| | |
|--|-----|
| Abstract | I |
| List of Figures | III |
| List of Tables | VI |
| 1 INTRODUCTION | 1 |
| 1.1 Overview | 1 |
| 1.2 Stretchable electronics | 1 |
| 1.3 Electrophysiological Recordings | 3 |
| 1.4 Chemical process for measurement | 3 |
| 1.5 Electrocardiogram (ECG) | 5 |
| 1.5.1 Electrocardiogram tracings | 5 |
| 1.6 Motivations and goals | 8 |
| 2 STATE OF THE ART | 9 |
| 2.1 Stretchable electronics in medical field | 9 |
| 2.2 Biopotential electrodes | 17 |
| 2.2.1 Wet-contact electrodes | 18 |
| 2.2.2 zPDMS/eGaIn electrodes | 19 |
| 2.2.3 cPDMS electrodes | 21 |
| 2.2.4 AgPDMS electrodes | 22 |
| 3 MATERIALS AND EQUIPMENT | 27 |
| 3.1 Materials | 27 |
| 3.1.1 Polydimethylsiloxane (PDMS) | 27 |

| | | |
|----------|--|-----------|
| 3.1.2 | Conductive materials | 29 |
| 3.1.3 | zPMDS | 29 |
| 3.1.4 | AgPDMS | 30 |
| 3.1.5 | Silver Epoxy | 32 |
| 3.1.6 | Liquid metal | 33 |
| 3.2 | Equipment | 34 |
| 3.2.1 | Laser cutter | 34 |
| 3.2.2 | T962C Reflow oven | 35 |
| 3.2.3 | Thinky ARE-250 mixer | 36 |
| 3.2.4 | ZUA 2000 Universal Applicator | 37 |
| 4 | FABRICATION METHODS | 39 |
| 4.1 | Circuit's design on PCB | 39 |
| 4.2 | Circuit's design on flexible PCB | 43 |
| 4.3 | Chips connection | 48 |
| 4.3.1 | Fixing of the chips | 48 |
| 4.3.2 | Fixing of the copper coated kapton sheet | 50 |
| 4.4 | Resistors and capacitors connection | 52 |
| 4.4.1 | Test with Silver Epoxy | 52 |
| 4.4.2 | Test with zPDMS | 53 |
| 5 | RESULTS | 55 |
| 5.1 | ECG with no flexible PCB | 55 |
| 5.1.1 | Wet-contact electrodes | 56 |
| 5.1.2 | zPDMS electrodes | 57 |
| 5.1.3 | AgPDMS electrodes | 58 |
| 5.2 | BPM comparision | 59 |
| 5.3 | Stretchable circuit | 60 |
| 5.3.1 | Chips connection | 61 |
| 5.3.2 | Resistors and capacitors connection | 62 |
| 5.4 | Final circuit | 62 |
| 6 | GENERAL CONCLUSION | 67 |
| 6.1 | Future Work | 68 |

| | |
|----------------------------|----|
| Appendix | 69 |
| A Programming code Arduino | 71 |
| B Programming PSoC creator | 79 |
| Bibliography | 89 |
| Acknowledgements | 91 |

Abstract

The development of stretchable bio-monitoring patch borns to facilitate the use of the, device through portability and adaptability, in this thesis, the device was created to facilitate the measurement of heart rate. Recent advances in flexible and stretchable electronics show great potential for wearable bioelectronics and epidermal sensor systems that are in contact with the surface of the human skin, for example for measuring physiological signals in diagnostics, and health and fitness monitoring applications.

The investigation of stretchable materials that can afford high electrical conductivity is demanded for such devices, and new challenges such as how to interface these soft systems with rigid components, how to deliver and store energy in them and how to take advantage of such structures to measure biological signals emerged. Although biological signal sensing is already a well studied field, current state of the art electrodes exhibit limitations from the user's comfort point of view - when considering long term applications - and biomonitoring devices are generally composed of hard, rigid and brittle hardware, far from being adequately conformable to soft human tissue. The development conformal and thus comfortable biomonitoring devices is, therefore, of great interest for several applications such as remote health monitoring, human-machine interface (HMI) devices and prosthetics.

This thesis aims to explore the fabrication of stretchable soft material circuit and biomonitoring patches, integrated in the current state of the art fabrication methods for stretchable electronics. The materials used are based in medical graded polymer - polydimethylsiloxane (PDMS) - a well known biocompatible elastomer, widely used in biomedical applications. The work further characterizes the methods of the product circuit and the different types of electrodes. This includes a series of novel electrodes composed of a medical graded silicone as the base polymer, mixed with conductive particles, compared against each other and reference commercial electrodes.

As a case study, the activity of non-invasive heart rate - electrocardiogram (ECG) - was acquired using AgPDMS electrodes. To do this it was necessary to deepen

the study on flexible PCBs together with their integration and that of other components on the stretchable circuit. Excellent results have been obtained in terms of signal reliability and heart rate (BPM) values, completely equal to the real values. In addition, important goals for the future have been achieved for the production of multilayer stretchable circuits.

List of Figures

| | | |
|------|---|----|
| 1.1 | Body conformable biomonitoring device | 2 |
| 1.2 | Deformability and stretchability | 2 |
| 1.3 | Commercial electrodes | 3 |
| 1.4 | Heart process's | 4 |
| 1.5 | Heart rate | 7 |
| 1.6 | ECG waves | 7 |
| | | |
| 2.1 | Biopotential electrodes | 10 |
| 2.2 | Study by Cotton and collaborators | 13 |
| 2.3 | Study by Lipomi and collaborators | 14 |
| 2.4 | Examples of structure solutions | 15 |
| 2.5 | Serpentine interconnection strategy | 16 |
| 2.6 | Expandable catheter | 17 |
| 2.7 | Biopotential electrodes | 18 |
| 2.8 | zPDMS electrode fabrication | 20 |
| 2.9 | zPDMS electrodes | 21 |
| 2.10 | cPDMS electrode fabrication | 22 |
| 2.11 | cPDMS electrodes | 23 |
| 2.12 | AgPDMS electrode fabrication | 24 |
| 2.13 | AgPDMS electrodes | 25 |
| | | |
| 3.1 | Polydimethylsiloxane | 28 |
| 3.2 | zPDMS z-axis | 29 |
| 3.3 | AgPDMS characterization | 31 |
| 3.4 | AgPDMS characterization | 31 |
| 3.5 | Liquid metal | 33 |

| | | |
|------|--|----|
| 3.6 | Laser | 34 |
| 3.7 | Material | 35 |
| 3.8 | T962C Reflow oven | 35 |
| 3.9 | Thinky ARE-250 | 36 |
| 3.10 | ZUA 2000 Universal Applicator | 38 |
| | | |
| 4.1 | MAX30003's chip | 40 |
| 4.2 | Logic level converter | 40 |
| 4.3 | Circuit's schematic | 41 |
| 4.4 | Eagle's design and PCB | 42 |
| 4.5 | CYBLE-022001-00 module | 43 |
| 4.6 | Circuit with one layer | 43 |
| 4.7 | Electrodes's position | 44 |
| 4.8 | Circuit with one layer (flexible) | 44 |
| 4.9 | Circuit with two layer | 45 |
| 4.10 | Separate circuit layers | 45 |
| 4.11 | Fabbrication of first layer | 46 |
| 4.12 | Circuit's fabbrication | 47 |
| 4.13 | Preparation of the second layer | 47 |
| 4.14 | Final circuit | 48 |
| 4.15 | Copper coated kapton sheet | 48 |
| 4.16 | Chip's CAD | 49 |
| 4.17 | Fabbrication chip | 49 |
| 4.18 | Chips on the flexible PCBs | 50 |
| 4.19 | Fabbrication test for the chip | 50 |
| 4.20 | zPDMS on top of the test circuit | 51 |
| 4.21 | PCB on the zPDMS | 51 |
| 4.22 | Fixing of the PCB with mistake and not | 52 |
| 4.23 | Siver Epoxy test | 53 |
| 4.24 | Final test circuit for zPDMS | 53 |
| | | |
| 5.1 | CY8CKIT-042-BLE-A chip configuration | 56 |
| 5.2 | Results with wet-contact electrodes | 56 |
| 5.3 | zPDMS electrodes for measurement | 57 |

| | | |
|------|--|----|
| 5.4 | Results with zPDMS electrodes | 58 |
| 5.5 | Results with AgPDMS electrodes | 59 |
| 5.6 | Final circuit measurements | 60 |
| 5.7 | PCB - circuit measurements | 61 |
| 5.8 | Resistors measurements | 62 |
| 5.9 | Connection with resistors | 63 |
| 5.10 | Chip placement | 64 |
| 5.11 | Complete circuit (top view) | 64 |
| 5.12 | Complete circuit (bottom view) | 65 |
| 6.1 | Flexible double layer PCB | 68 |

List of Tables

| | | |
|-----|---|----|
| 3.1 | Typical material properties of PDMS | 28 |
| 3.2 | ZUA 2000 Universal Applicator technical specification | 38 |
| 4.1 | Arduino's connections | 42 |
| 5.1 | Standing comparison table | 59 |
| 5.2 | Sitting comparison table | 60 |

Chapter 1

INTRODUCTION

1.1 Overview

Stretchable electronics received an increasing attention during the last decade due to their applications in sensing, wearable computing, biomonitoring and conformal Human Machine Interfaces (HMIs). This chapter briefly describes the main principles behind stretchable electronics, focusing on thin film stretchable sensors and their role in wearable electronics. Being ECG sensing the main focus of this thesis, the basic principles of electrophysiology are also introduced. Finally, the motivations and goals of the project are presented, as well as a brief overview of the thesis.

1.2 Stretchable electronics

There has been an on-growing demand for stretchable devices since the birth of new technology fields like stretchable electronics, intelligent soft robotics and wearable and body conformable devices. Materials that can afford high electrical conductivity, while also having a good combination of mechanical properties such as stretchability, toughness and tear resistance are, therefore, required. This rapidly uprising area led researchers to face new challenges such as how to interface soft electronics with rigid components, how to deliver and store energy in them and how to take advantage of such structures to measure bio-signals.

This dissertation focuses on the application of state of the art materials and fabrication methods to produce wearable and body conformable biomonitoring devices

(1.1), taking advantage of thin film stretchable sensor technology.

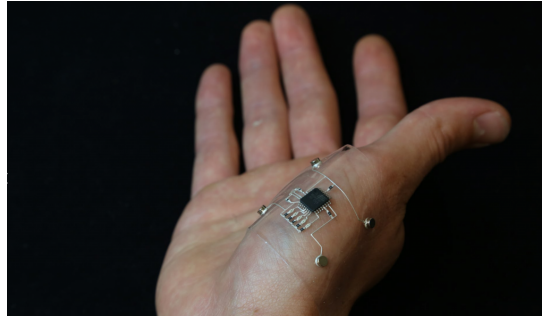


Figure 1.1: Body conformable biomonitoring device [6].

Traditional sensors and electrical components are generally rigid and best suited to systems of discrete motions and confined trajectories (used in the field of industrial robotics, for instance). Soft structures, however, have more degrees of freedom than rigid systems, due to their deformability (1.2), and thus require their surface to be populated with thin film stretchable structures with embedded sensing components. These sensors must be mechanically compatible and conformable with their target: in the case of human skin, it is required that the sensor can undergo at least a 20 % [11].

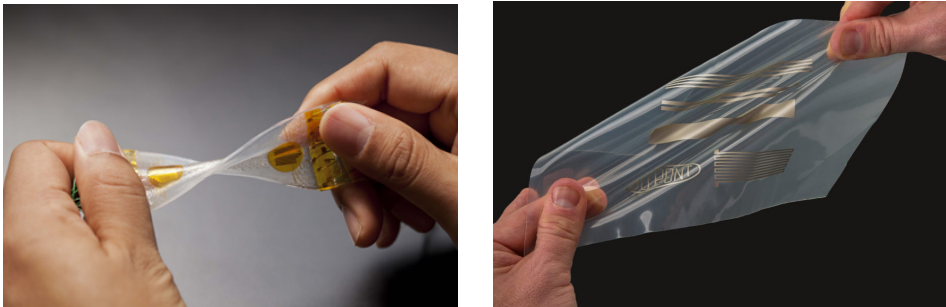


Figure 1.2: Deformability [5] and stretchability [6].

Such sensors' applications range from the area of soft robotics (for robots' proprioceptive feedback) to biomedical applications. Wearable biomonitoring is a step towards the reduction of hospital care costs and increase of patients' independence and comfort by limiting the number of unnecessary hospital visits. But the monitoring of body-derived physiological information is not only limited to medical applications: sports, ergonomics and human-machine interfaced devices (HMIs) - like prosthetics

- are some of the other areas that profit with the technology. The signals sensed by such devices include heart and breath rate, temperature, sweat components (like glucose or cortisol) or the focus of this thesis: biopotentials (electrophysiological recordings) [21].

1.3 Electrophysiological Recordings

Bioelectric phenomena can be found in just about every organ system of the body. Nervous stimuli and muscle contractions can be detected, using biopotential electrodes that measure the ionic current flow in the body. A biopotential electrode is a transducer that senses ion distribution on the surface of the skin and converts it to electric current. Traditionally, silver/silver-chloride (Ag/AgCl) electrodes combined with wet conductive gels have been widely used (1.3).



Figure 1.3: Commercial electrodes

But in this thesis we will discuss also other types of electrodes which, by the way they are produced, better adapt to the type of device to be produced for their elasticity, deformability, resistance and adaptability to the human body.

1.4 Chemical process for measurement

A bioelectric potential is a result of the electrochemical activity of certain cells known as excitable cells, which compose nervous and muscular tissue. These cells exhibit a steady electrical potential difference between their internal and external

environments, known as the resting potential (between 40 and 90 mV in the internal medium, relative to the external medium, depending on the cell type). At this state, the membrane of the cell is more permeable to K^+ ions than Na^+ , and the internal concentration of K^+ is much higher than the exterior. Therefore, a diffusion gradient of K^+ occurs towards the exterior of the cell, making the interior more negative in relation to the exterior, resulting in an electrical field built up towards the interior of the cell. Ultimately, the diffusional and electrical forces that act across the membrane are opposed to one another, and a balance is achieved at the *polarization voltage* or *resting potential* [15, 29].

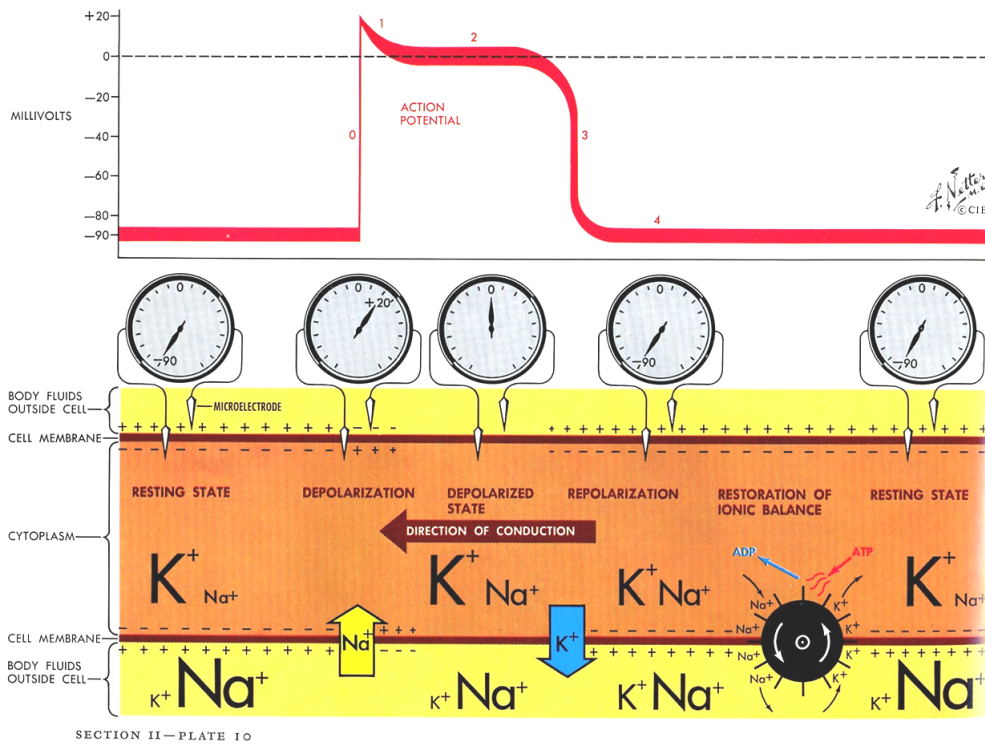


Figure 1.4: Heart process's [2].

When the excitable cell is electrically stimulated by the central nervous system, the permeability to Na^+ ions increases, thus making these ions to diffuse toward the interior of the cell, leading to an intracellular potential increase called depolarization. As this potential reaches a certain positive value, the permeability of the membrane decreases for Na^+ ions and increases for K^+ ions, causing the membrane potential to return to its resting state - repolarization. This cycle of the cellular potential

is called action potential (1.4): the electrophysiological signals (such as the ECG, EMG and EEG) are the result of a combination of different cells producing action potentials [15, 18].

1.5 Electrocardiogram (ECG)

Cardiac contractions are accompanied by a change in the electrical potential of heart muscle cells. These changes are reflected in the current and in the electrical potential present in the body and can be recorded on the epidermis. The method used to measure and record these potential differences is called the electrocardiogram or ECG.

During each beat, in an orderly progression, waves of depolarization start from the pacemaker cells in the sinoatrial node, spread through the atria, pass through the atrioventricular node and continue in the bundle of His and in the fibers of the Purkinje, which extend down and left, hugging both ventricles. This orderly model of depolarization gives rise to the characteristic pattern of the electrocardiogram. Since the heart cells do not undergo simultaneous depolarization and repolarization, the appearance of the ECG has a particular shape, completely different from the recordings of a single cell or a small group of cells. The appearance of the waves is determined by the electric state present in the electrodes positioned in the different parts of the body. An upward shift is called positive, a negative downward direction. The vertical extension or amplitude of the displacement will be greater as the electrical potential is greater: therefore the vertical amplitude represents the intensity of the present electrical potential.

The electrocardiogram is a simple and safe basic test, used in many clinical contexts: to measure the frequency and rhythm of heartbeats, to check the size and position of the heart chambers, to detect the presence of possible damage to the myocardium or to the conduction system, or control the effects of drugs and the good functionality of a pacemaker.

1.5.1 Electrocardiogram tracings

The principle on which the measurement of the electrical activity of the heart is based is purely physiological: the onset of impulses in the myocardium leads to the

generation of potential differences, which vary in space and time and which can be recorded by means of electrodes. The electrocardiographic trace represents the easiest, least expensive and most practical method to observe if the electrical activity of the heart is normal or if there are pathologies of a mechanical or bioelectrical nature. The normal ECG pattern has a characteristic appearance: the path is characterized by different traits called waves, positive and negative, which are repeated at each cardiac cycle.

The ECG is composed of positive waves (P, R, T) and negative (Q, S), the positivity or negativity is referred to the isoelectric line, which is the baseline of the electrocardiogram (1.5).

- Wave P: is the first wave that identifies itself in the cycle. Corresponds to the depolarization of the atria, it originates from the sinoatrial node and the vector thus originated is oriented downwards and to the left.
- PQ interval: the wave front, through the atria, passes into the atrioventricular node within which the activated cells are few and the dipole generated is too weak to be recorded.
- QRS complex: it is a set of three waves that follow one another, corresponding to the depolarization of the ventricles. The wave Q is negative, of small dimensions, and corresponds to the depolarization of the interventricular septum, the product vector is directed from left to right; the wave R is a very high, positive peak, corresponding to the depolarization of the apex of the left ventricle and so evident, because it is linked to the particularly relevant muscle mass; the wave S is a negative wave, also of small dimensions like the Q, and corresponds to the depolarization of the basal and posterior regions of the left ventricle.
- ST Tract: represents the period in which the ventricular cells are all depolarized and therefore no electric movements are detectable, until the beginning of the repolarization; it follows that, as a rule, the ST segment is isoelectric, ie placed on the base line of the track.
- Wave T: represents the first wave of the repolarization of the ventricles. It is not always identifiable, as it can be very small in size.

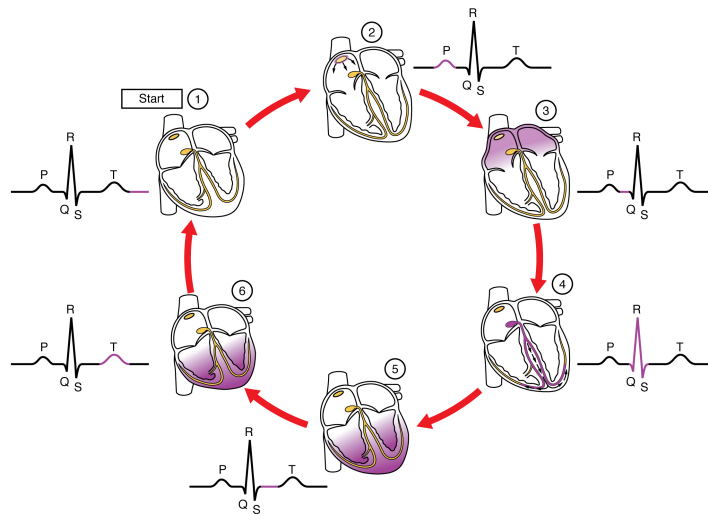


Figure 1.5: Cardiac Conduction. (1) The sinoatrial (SA) node and the remainder of the conduction system are at rest. (2) The SA node initiates the action potential, which sweeps across the atria. (3) After reaching the atrioventricular node, there is a delay of approximately 100 ms that allows the atria to complete pumping blood before the impulse is transmitted to the atrioventricular bundle. (4) Following the delay, the impulse travels through the atrioventricular bundle and bundle branches to the Purkinje fibers, and also reaches the right papillary muscle via the moderator band. (5) The impulse spreads to the contractile fibers of the ventricle. (6) Ventricular contraction begins [14].

Considering the ECG trace, one can easily obtain the heart rate by evaluating the elapsed time between one cycle and the next, taking two successive "RR" peaks as a reference.



Figure 1.6: ECG waves [3].

1.6 Motivations and goals

The recording of physiological signals through the skin, whether in clinical or in any other application, is many times useful under dynamic conditions and / or for long-term periods. Conventional biopotential measurements use adhesive electrodes combined with an electrolytic paste and are often cited as irritating and uncomfortable for long-term monitoring, sometimes sometimes requiring complex skin preparation.

The alternative usage of dry electrodes has therefore gained its popularity. This condition requires the use of the skin and is highly susceptible to motion artifacts [13].

In addition to the electrodes, the current solutions for physiological signaling are composed of hard, rigid, and brittle hardware, such as electronic printed circuit boards (PCBs), which are not adequately conformable to soft human tissue and organs. Even the solution for continuous EMG monitoring, currently used for the control of prosthetics, is not ergonomic for long term wearing .

In an attempt to overcome the issues regarding current state of the art electrodes and wearable electronics, the goal of this dissertation is to evaluate the application of different sets of conformable stretchable electrodes and biomonitoring patches. Such electrodes' fabrication is based in a medical graded polymer - polydimethylsiloxane (PDMS) - which is not gel like as in current wet-contact electrodes, but at the same time is more flexible and stretchable than reusable rigid electrodes and, thus, more ergonomic. The work also explores how these electrodes can be integrated into state of the art fabrication methods of stretchable electronics, for skin-conformable biomonitoring patches in the future.

As a case study, it was opted to demonstrate heart rate detection, using sECG sensors based in such materials.

Chapter 2

STATE OF THE ART

In this chapter, the main types of state of the art about stretchable electronics and biopotential electrodes are reviewed, along with their strengths and weaknesses.

2.1 Stretchable electronics in medical field

These devices are able to actively monitor and manipulate the fabric with the level performance of an advanced microelectronic system and simultaneously enjoy the ability to accompany the fabric during the history of deformations resulting from its intrinsic vitality and interaction with the surrounding districts (as in the case of the myocardium): moreover, the dimensions of the individual sensitive and/or actuating units follow the principle of miniaturization because inherited from microelectronics, so it is realistic to assume that the extension of the whole device can be kept sufficiently small to admit a minimally invasive application [12]. It is no coincidence that the commitment of industry and academic research in the field of stretchable electronics has concentrated predominantly in solutions of great interest from the biomedical point of view, with particular attention to applications in which the level of performance is closely related to the effectiveness of the interface strategy with the fabric [12].

In a device belonging to the stretchable electronics category it is possible to recognize at least three fundamental elements:

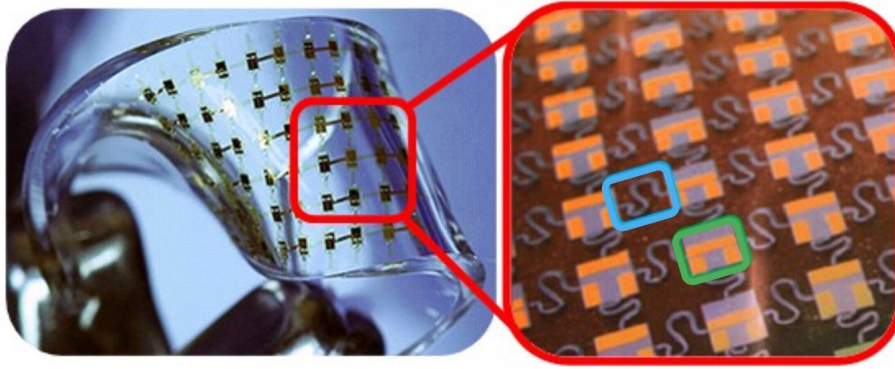


Figure 2.1: Example of a stretchable electronics device; a) Example of the high deformability of the polymeric matrix; b) Detail showing some replicas of rigid islands (green box) and corresponding interconnections (blue box) [12].

- The polymer matrix (2.1a), highly deformable in the native sense and used only for support or complete coating of the integrated circuit. In addition to making the system intrinsically deformable, this element is often responsible for the mechanism of redistribution of stresses on the circuit component: the objective is the safeguarding of electrical performances, otherwise incompatible with the presence of significant deformation regimes [12]. In fact, we speak of devices that must continue to be functional even after having undergone lengthening equal to 100% of their initial deformation [12];
- integrated circuits (2.1b, green box), which is responsible for measuring and/or implementing the device. In most cases, these elements are actually micro-devices obtained by means of Si-technology conventional, therefore on the one hand they constitute the regions in which the value of the device is concentrated from the electronic point of view, while on the other they represent the only rigid portion of the system [12]. For this reason the integrated circuits are arranged in the form of sensitive and/or active islands, each one separated from the others because it borders along the entire perimeter with the polymer matrix. This strategy allows to preserve the deformability of the device as a whole, but in order that all the integrated circuits can interact with each

other and/or with an external power supply and data collection system, it is essential that they are not isolated also from the electrical point of view [12];

- The interconnection (2.1b, blue box), which can be intrinsically deformable or can acquire this characteristic by virtue of a suitable structural design. Since this element has the same role as the electrical connection cable from a circuit point of view, the specifications of its competence are a low resistivity, constant and independent of deformation state in almost-static or eventually dynamic sense (in the case where the stress prescribed for the device is cyclic nature), from temperature and humidity [12].

Of these three elements, the polymer matrix and the interconnection are the main novelties from a design point of view between a macroelectronic device for stretchable electronics and a microelectronic product. Not only the choice of materials and their individual optimization respect to the role covered in the device, but the design of the correct coupling between the polymer matrix and the interconnection constitutes a central node in the study of devices for stretchable electronics, in which the electromechanical coupling plays a major role when defining the specifications [12]. In reality, in the devices of the stretchable electronics, the electromechanical problem is not to be considered a strong coupling as in the case of piezoelectric materials or electromechanical microsystems (MEMS): as a first approximation, it can be studied as a weak coupling in which the mechanical problem affects the electrical one, but not vice versa, and consequently the preliminary design of the device can be configured as the optimization of the mechanics on the matrix-interconnection system, with the aim of extending as far as possible the range of stress conditions in which to subject the system without altering the resistivity of the interconnection. This includes, for example, establishing the stresses beyond which the interconnection manifests a non-linear electrical characteristic or shows fracture phenomena which lead to the inability of the interconnection to transmit the electrical signal. The optimization, intended as the study of the mechanics of the device, does not completely exhaust the design, because the true performance of the system with respect to service conditions is described exhaustively only by the definition of a calibration curve, which provides the relationship between physical quantities that you want to measure in application (eg, temperature, deformation, electrical activity) and the corresponding electrical signal provided by the device: the research

groups involved in this sector, they accompany always the proposal of a device in its application version an electromechanical characterization or a validation and a calibration of the system [12].

Nevertheless, to predict the mechanical response of the device respect to the operating stresses is a crucial preliminary aspect, because it allows to verify and circumscribe the adequacy and applicability of the solution to the problem [12].

A fundamental aspect in the design of a device for flexible electronics is that any material shows flexibility if it is possible to obtain a replica with a sufficiently reduced thickness: applying this principle it is possible to obtain flexible and roll-up sheets of intrinsically fragile material. Examples are the flexible solar cells made by depositing Si with a thickness of about 100 μm on polymeric substrates. This justifies the typically structural nature of the flexible electronics design solutions, which tend to reduce the stresses on the electronic component by decreasing its flexural stiffness by thinning it or by encapsulating it in a polymer matrix and arranging it so that, subjected to service stresses, it is always in the neutral axis position of the whole system [12].

The study by Cotton and collaborators shows that a similar strategy can be adopted also in the field of stretchable electronics, but with limited applicability: the authors have created a pressure sensor placing two sets of straight golden conductors (Au) in form of thin films (thickness 50 nm, width 2 mm) on opposite sides of the same polydimethylsiloxane substrate (PDMS, thickness 500 nm) (2.2) [12].

In this configuration, the PDMS functions simultaneously as highly deformable and dielectric polymer substrate, the capacitive elements are formed by the overlapping regions of the thin films of Au and the same act as interconnections along the rest of their development. The device, proposed as an example of artificial skin, has demonstrated satisfactory performances measuring with reliability pressures until to 160 kPa and deformations up to 20%, considered typical of the epidermal tissue. However, the applications of the stretchable electronics involve higher deformations, which can not be achieved by using a thin conductive film as interconnection [12]. Alternative strategies can be divided into two main categories::

- **Material oriented approaches:** in this case we try to combine the high

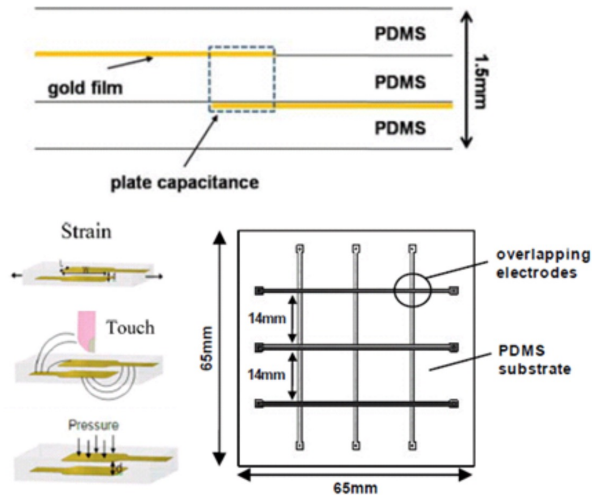


Figure 2.2: Schematic representation of the device made by Cotton and collaborators [12].

deformability with electrical performances by designing a new and unconventional material, intimately capable of simultaneously manifesting both characteristics. This corresponds to making conductive elastomeric insulating substrates (PDMS, polyurethane) by including particles of conductive material (eg, Fe, Al, Cu, C): it has been shown that it is possible to identify a volumetric fraction value of filler (percolation threshold) beyond which the heterogeneities are so numerous and close to entering in mutual contact, forming a continuous network and conferring conductivity to the resulting composite. The study of Lipomi and collaborators, who have created a matrix of capacitive sensors in exactly the same way as described for Cotton, realizing on PDMS a deposition with parallel bands of carbon nanotubes (CNT) where there are film sets thin of Au [12].

The sensitive membrane obtained (2.3) has shown a linear dependence of the capacity for pressures until to 50 kPa and for deformations until to 50%, allowing a considerable gain in terms of deformability of the system, but suffering, however, some critical issues such as: the resistivity of conductive elastomers usually high and electrical behavior of the conductive elastomers results from the complex interactions between the heterogeneities dispersed in the insulating matrix [12].

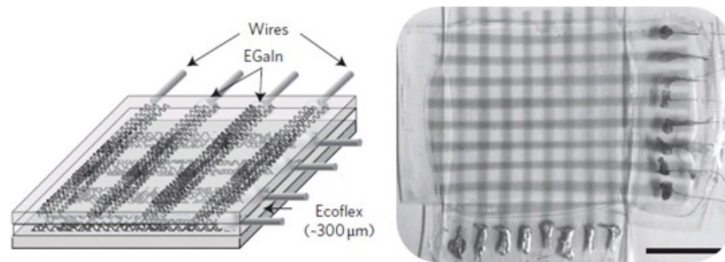


Figure 2.3: Schematic representation (left) and photography (right) of the device realized by Lipomi and collaborators [12].

- **Structure oriented approaches:** contrarily the previous one, this strategy favors the use of conventional materials and focuses on the identification of structural measures more sophisticated than those proposed by flexible electronics, with the aim of making more deformable those materials that are not intimately.

A first example consists in depositing the conductive thin film maintaining the polymeric substrate in a condition of moderate biaxial *pre-stretch* (e.g., 10-20 %): finished the deposition phase, the compressive stresses which arise for effect to the release of the polymer substrate induce in the conductive film a phenomenon of instability typical of the beams and of the thin plates, due to which the surface of the film assumes typically a shape wavy, usually defined *ribbon* (2.4a). Scientific results show that, for induced *buckling*, an interconnection thus obtained assumes the ability to sustain elongations even higher than the value of *pre-stretch* imposed during deposition [12].

A natural evolution of this strategy consists in refining the deposition technique on the *pre-stretch* substrate by imposing that the bond between it and the conductive film is selectively realized in some regions, leaving the rest of the free interconnection to rise during the substrate withdrawal the structural arrangement thus obtained is called *open-mesh* and the interconnection portions raised from the plane are called *bridges*(2.4b).

This technique has been adopted by Lee and his collaborators to make deformable thin films (300 nm thickness) semiconducting of Si and gallium arsenide (GaAs): despite of the native fragility of these materials, as reported

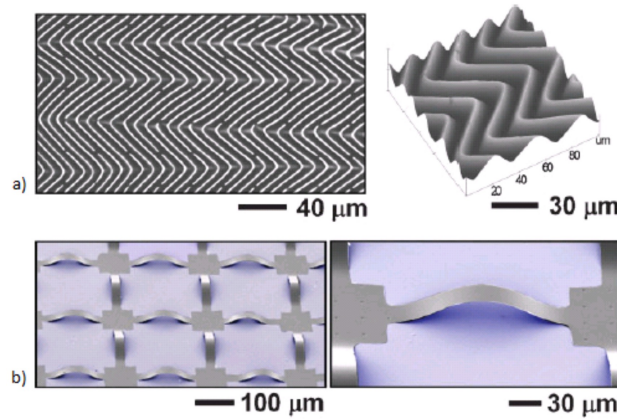


Figure 2.4: Examples of solutions oriented to the structure: a) *ribbon* structure; b) *open-mesh* structure [12].

by the authors, the devices thus obtained they are capable of reversibly supporting deformations equal to 100% [12].

A significant improvement is certainly due to the important mechanism by which the macroscopic deformation is locally redistributed due to the structural order imposed: the first deformation phases do not directly involve the interconnection material, but they do it indirectly by imposing the bridges to reduce its deflection; in these circumstances, the interconnection is mainly in *bending* (flexion) and being a thin plate from the structural point of view, its reduced bending rigidity ensures that the stresses and strains locally experienced by the material are contained. In the literature, the phenomenon according to which the macroscopic deformation is entrusted to the structural design rather than directly to the interconnection is often referred to as *isolation of the deformation* [12]. In the specific case of open-mesh structures, the strategy is a method to transforming what locally is a structural device inherited from flexible electronics, so an increase in flexibility, in an increase of the device deformability in a macroscopic sense [12].

Although this solution is very promising, the application of a pre-stretch during the deposition step and the creation of a bond with the substrate limited to specific regions makes the manufacturing procedure of these devices more complex and expensive. For this reason, some research groups have sought an alternative in the realization of metallizations with planar serpentine shaped

(2.5) [12].

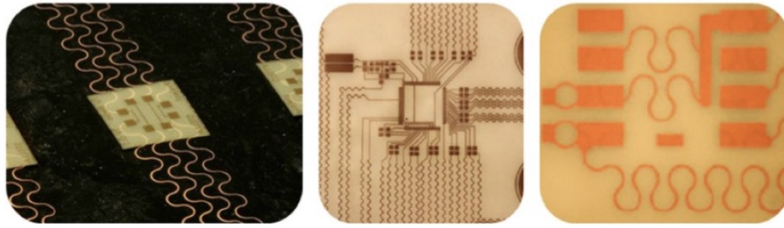


Figure 2.5: Examples of stretchable electronics devices in which the serpentine interconnection strategy has been used [12].

This solution has a double advantage:

1. being a planar pattern and not referring to the *buckling* strategy induced, is compatible with conventional micro-manufacturing techniques.
2. the deformation isolation mechanism associated with the use of a serpentine design is significantly more effective.

From an application point of view in the biomedical sector, the technique of serpentine interconnections has been successfully adopted by Kim and collaborators to equip an expandable catheter with a set of sensors and actuators and enable their use for cardiac ablation with radiofrequency (2.6), a procedure indicated in case of alterations in the synchrony of the electrical activity of the heart (ie, *cardiac arrhythmias*): this device is a unique example of its kind and shows perfectly how the stretchable electronics can be integrated into conventional surgical instruments (in this case interventional), enriching them with added value [12].

The effectiveness of this device has been experimented by the authors on an animal model, in particular on rabbit hearts: to simplify the evaluation of the device performance, in this preliminary study the expandable catheter was tested on the epicardium surface, followed by sternotomy (2.6, left column) [12].

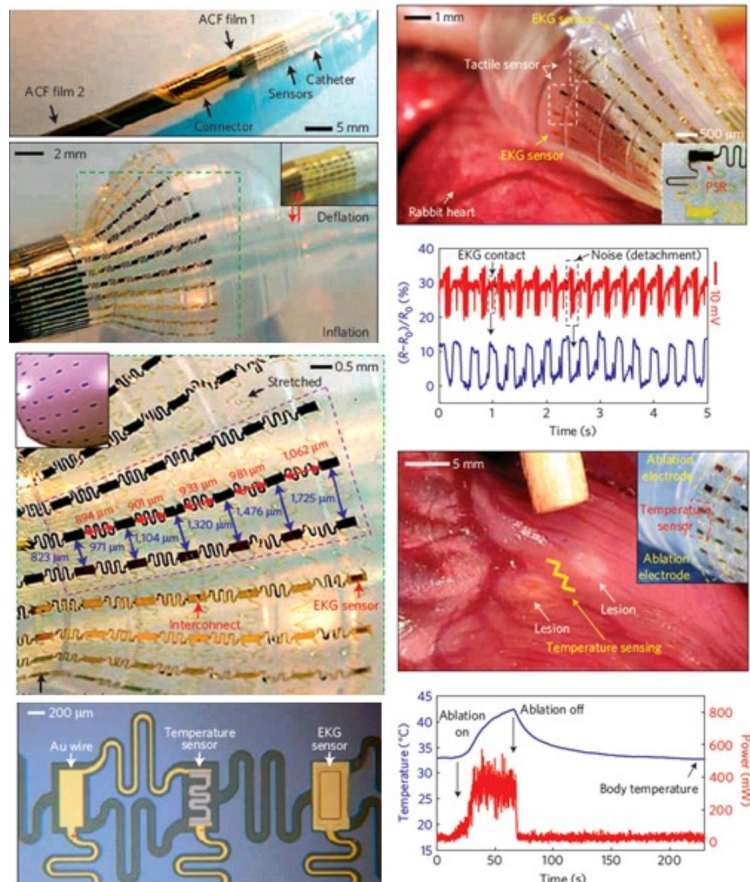


Figure 2.6: Expandable catheter equipped with sensors and active electrodes by Kim and collaborators. In the left column it is possible to observe in more detail the integrated sensors on the catheter, in the right hand column some examples some example of electrocardiographic and temperature measurements have been reported obtained in the experimental site of the device [12].

2.2 Biopotential electrodes

The mechanism of electric conductivity in the body involves ions as charge carriers. Thus, picking up bioelectric signals involves interacting with these ionic charge carriers and transducing ionic currents into electric currents required by wires and electronic instrumentation [22]. This transducing function is carried out by electrodes that consist of electrical conductors in contact with the aqueous ionic solutions of the body [22]. The interaction between electrons in the electrodes and ions in the body can greatly affect the performance of these sensors and requires that specific

considerations be made in their application [10].

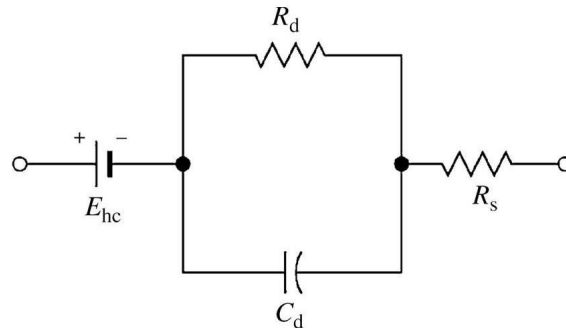


Figure 2.7: Equivalent circuit for a biopotential electrode in contact with electrolyte E_{hc} is the half-cell potential, R_d and C_d make up the impedance associated with the electrode-electrolyte interface and polarization effects, and R_s is the series resistance associated with interface effects and due to resistance in the electrolyte [22].

Exist four different types of electrodes:

- Wet-contact
- zPDMS/eGaIn
- cPDMS
- AgPDMS

2.2.1 Wet-contact electrodes

An electrolyte solution (or gel) is traditionally placed on the side of the electrode that comes in contact with the skin, which absorbs it, decreasing the recording impedance. A chemical reaction occurs at this interface: current passes from the electrolyte to a non-polarized electrode, oxidizing its atoms to form cations and electrons [23, 24]. The cations discharge into the electrolyte, as the electrons carry charge through lead wires connected to the electrodes. The anions in the electrolyte also deliver free electrons to the electrode and a voltage known as half-cell potential is generated across the interface as a result of an uneven distribution of anions and cations [23, 24].

Silver/silver chloride (Ag/AgCl) electrodes are the traditional choice regarding this

electrode type, due to their low half-cell potential and ease of manufacturability. They are non-polarizable, meaning that current is allowed to pass across the interface between the electrolyte and the electrode, which introduces less electrical noise into the measurement [16]. The standard wet Ag/AgCl electrode is still almost universally used for clinical and research applications: while problematic from a patient comfort standpoint, adhesive wet electrodes adhere very well to the skin, staying fixed to specific, clinical-standard locations on the body. These electrodes are most commonly disposable (1.3) [16, 24].

2.2.2 zPDMS/eGaIn electrodes

The fabrication of zPDMS/eGaIn electrodes is based on two of the methods: laser patterning and spray deposition.

1. A laser cutter may be used not only for stencil patterning, but also for direct polymer patterning. The first step of this method is to cast and cure a film of PDMS or PDMS composite on a substrate. After that, the sample is taken to the laser to be cut in the desired pattern, previously drawn in a compatible software. The power and speed that should be programmed for the laser may vary depending on the thickness of the film to be cut; it is desired that the sample is cut all the way through, so that the excess may easily be removed manually afterwards [21].
2. Spray deposition is a method used in this work to pattern liquid metal traces. It requires the usage of a spray gun, with its recipient filled with the liquid metal (eGaIn). The method shows better uniformity and dispersion of the eGaIn particles and consumes less material than other known methods, such as roller deposition. This fabrication method is useful when combined with the use of stencils to pattern the liquid metal. As such, similarly to the stencil lithography method, the first steps consist on casting and curing a base layer and placing the stencil above. The sample is then sprayed with eGaIn, which will adhere to the patterned shape, and finally the stencil is removed, leaving the desired pattern on the sample. A top layer of PDMS must be cast and cured over the sample, so that the liquid metal is encapsulated [21].

The fabrication steps are the following:

- Deposition and curing of a $250\ \mu\text{m}$ PDMS layer, using the thin film applicator (a);
- Laser patterning of the electrode areas and removal of the excess PDMS (b);
- Deposition and curing of a $250\ \mu\text{m}$ zPDMS layer to fill the PDMS gaps, using the thin film applicator (c);
- Stencil placement over the sample (d);
- Liquid metal spray deposition over the sample and removal of the stencil (e);
- Deposition and curing of a $250\ \mu\text{m}$ PDMS layer, using the thin film applicator, to encapsulate the liquid metal (f).

The figure (2.8) shows a schematic diagram of the zPDMS electrode fabrication.

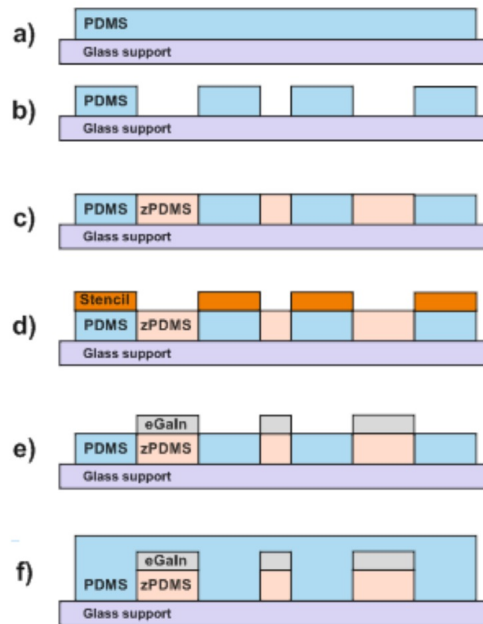


Figure 2.8: Side-view scheme of the zPDMS electrodes' fabrication steps [21].

The thickness chosen for each layer is an empirical solution for the fabrication of these electrodes. Using thinner layers, above or below the liquid metal, may reduce the robustness of the sensor, making it more fragile. Using thicker layers, on the other hand, increases the overall size of the sensor, which is also unwanted;



Figure 2.9: Top view (left) and bottom view (right) of the final zPDMS electrodes [21].

besides, a thicker layer of zPDMS on the bottom may lead to smaller sensitivity of the electrodes (since the conductivity of zPDMS changes according to the thickness) [21].

2.2.3 cPDMS electrodes

cPDMS is the name given to the mixture of PDMS with *Carbon Black powder*. Carbon Black particles are widely used to incorporate conduction to polymer composites, mainly because of their much greater tendency to form a conductive network due to their chain-like aggregate structures compared with other conductive additives such as metal powder [30]. Like many conductive polymer composites, cPDMS exhibits percolation characteristic, meaning that for a certain interval of filler concentration values, conductivity increases drastically for small increments of concentration: for cPDMS, that interval starts at approximately 15 wt%. The use of concentrations higher than 22 wt%, however, makes the sample very difficult to mix and cast.

Said that, cPDMS electrodes' fabrication doesn't require the use of liquid metal and, as such, skips the spray deposition method. The fabrication steps are the following:

- Deposition and curing of a 450 μm PDMS layer, using the thin film applicator (a);
- Laser patterning of the electrode areas and removal of the excess PDMS (b);
- Stencil placement over the sample (c);

- Deposition and curing of a $500\ \mu\text{m}$ cPDMS layer, using the thin film applicator (d).

The figure (2.10) shows a schematic diagram of the cPDMS electrode fabrication.

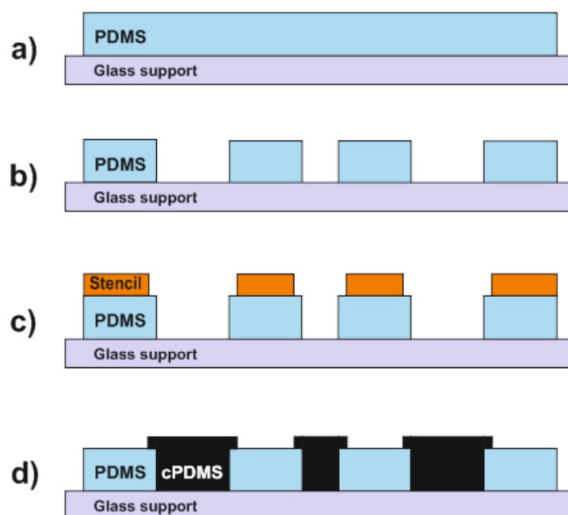


Figure 2.10: Side-view scheme of the cPDMS electrodes' fabrication steps [21].

For cPDMS electrodes, the initial PDMS layer is cast with a bigger thickness ($450\ \mu\text{m}$) than for zPDMS/eGaIn electrodes, and the cPDMS is patterned with a thickness of $500\ \mu\text{m}$, so that cPDMS traces of $50\ \mu\text{m}$ come on top of the PDMS layer [21]. That way, the final structure has the same thickness for both sensors ($500\ \mu\text{m}$), considering that the top layer cast for the zPDMS/eGaIn electrodes is not necessary for this case (cPDMS can be exposed, as opposed to liquid metal) [21]. The stencil used to pattern the cPDMS in c) should have the electrode areas slightly bigger than the ones used to pattern the PDMS in b), to make sure the interfaces between PDMS and cPDMS don't collapse when removing the final structure from the glass support [21].

The final result is in the figure below (2.11).

2.2.4 AgPDMS electrodes

Silver (Ag) has been of particular interest in PDMS composite electrodes due to its desirable wetting properties and suitability for biological applications. Ag yields the



Figure 2.11: Top view of the final cPDMS electrodes [21].

lowest interfacial impedance, compared to other metals such as titanium and copper, which is important for minimizing signal distortion [28]. Ferromagnetic metals such as nickel have been shown to induce a magnetic field that can affect electrical measurements while silver does not cause such complications. AgPDMS electrodes have previously been used in several applications. For instance, AgPDMS was used in temperature-dependent devices, such as a microheater and thermochromics display [28]. AgPDMS conductivity also varies as a function of strain, showing potential as a pressure sensor. Finally, AgPDMS has been used in droplet detection applications, where impedance signals reflect droplet size. Despite these applications, AgPDMS electrodes have not yet been investigated for performing impedance spectroscopy [28].

Impedance spectroscopy is a useful technique for measuring the electrical properties of cells, including size and size-independent quantities such as cytoplasm conductivity and specific membrane capacitance. In this technique, the cell is typically modeled as a single-shelled sphere. The cell membrane is represented as a thin dielectric shell, which contains the homogeneous resistive cytoplasm [28].

AgPDMS composite was fabricated and used to form electrodes for impedance measurement, in fact it is capable to measure cytoplasm conductivity and specific membrane capacitance of single cells.

The fabrication steps are the following:

- Glass support where I make the electrodes (a);
- Put on the top the stencil to be cut to give the desired shape of the electrode (b);
- Cut with the laser the stencil and depose of a 250 μm AgPDMS layer to fill the stencil gaps, using the thin film applicator (c);
- Remove the stencil from glass support (d);
- Deposition and curing of a 250 μm PDMS and AgPDMS layers, using the thin film applicator, and put it in the oven at 150° (e);
- Finally remove the support glass (f).

The figure (2.12) shows a schematic diagram of the single cell impedance measurement system.

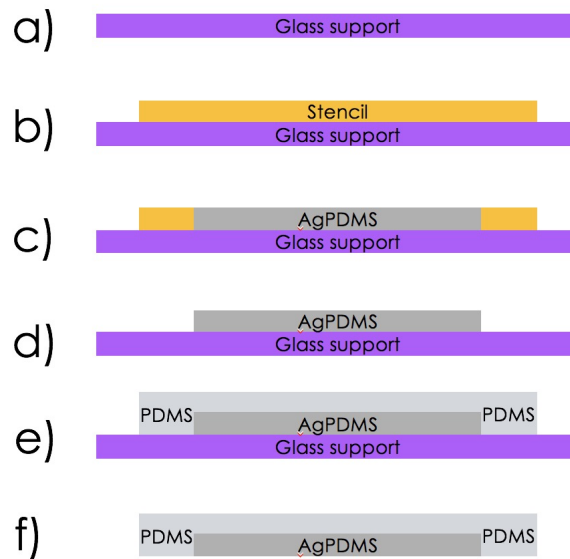


Figure 2.12: Side-view scheme of the AgPDMS electrodes' fabrication steps.

The final result is in the figure below (2.13).

Fabricating AgPDMS electrodes required the determination of adequate Ag concentrations (21 vol%) and in my work, I found that AgPDMS is non-conductive at 69 wt% and has excellent conductivity at 85 wt%.

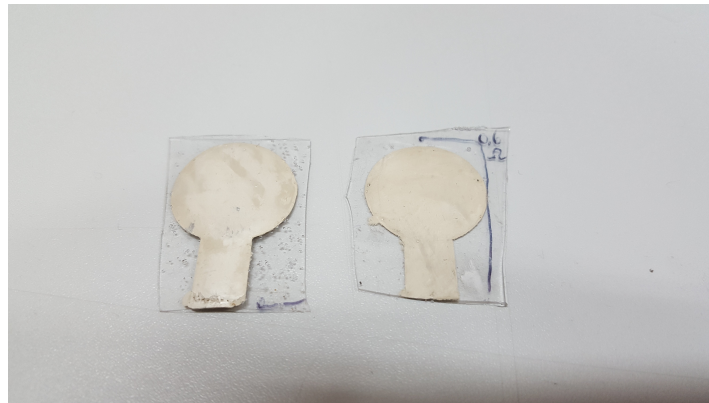


Figure 2.13: AgPDMS electrodes

For this reason I choose this material to make the final electrodes and to receive the heart signal.

Chapter 3

MATERIALS AND EQUIPMENT

3.1 Materials

In this chapter, the materials and equipment used along the course of this project to fabricate stretchable circuit and bio-monitoring patches are summarised.

Since the focus is on elastomeric-based sensors, the "Materials" section is divided in two parts: the non-conductive elastomeric substrate used (PDMS) and the remaining conductive materials, which carry both the functions of biopotential sensing and electrical information conveying (interconnecting).

3.1.1 Polydimethylsiloxane (PDMS)

Polydimethylsiloxane (PDMS) is a silicon-based organic polymer. In the development of this project, it was produced using a commercially available two-part kit by *Dow Corning* named *Sylgard 184*. The two components of the kit are the polymer's monomers and the curing agent, meant to be mixed in a weight proportion of 10:1, respectively. After the mixing process, PDMS just needs to be cast in the desired pattern and cured, either at room temperature (which can take up to 12 hours) or in an oven/hot plate at 180°C for approximately 8 minutes.

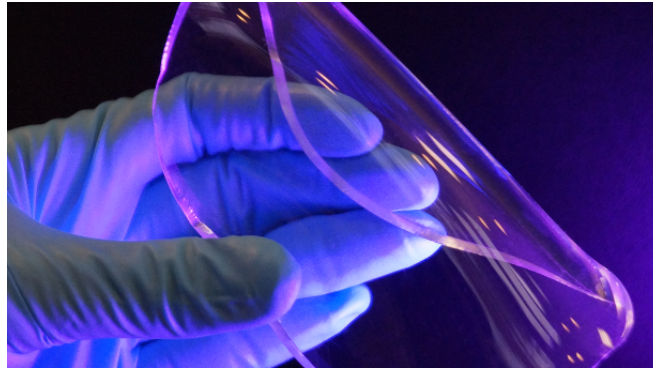


Figure 3.1: Polydimethylsiloxane (PDMS) [1].

PDMS is a transparent, chemically inert, thermally stable, gas and moisture permeable silicone with high elastic deformability. It is furthermore simple to handle, manipulate and produce, as described previously. For these reasons, it has become one of the most widely used materials in many biological or biomedical applications. Also, for their very low electrical conductivity, polymers like PDMS can act as electrical insulators. More recently, material designers started to blend insulating polymers with conductive ingredients to make them electrically conductive.

| Property | Value |
|--|---|
| Glass transition temperature (T_g) | $\approx -125^\circ\text{C}$ |
| Mass density | 0.97 kg/m^3 |
| Young's modulus | 360–3000 kPa |
| Poisson ratio | 0.5 |
| Tensile or fracture strength | 2.24 MPa |
| Specific heat | 1.46 kJ/kg K |
| Thermal conductivity | 0.15 W/m K |
| Dielectric constant | 2.3–2.8 |
| Index of refraction | 1.4 |
| Electrical conductivity | $4 \times 10^{13} \Omega\text{m}$ |
| Magnetic permeability | $0.6 \times 10^5 \text{ cm}^3/\text{g}$ |
| Wet etching method | Tetrabutylammonium fluoride ($\text{C}_{16}\text{H}_{36}\text{FN}$) + <i>n</i> -methyl-2-pyrrolidinone ($\text{C}_5\text{H}_9\text{NO}$) 3:1 |
| Plasma etching method | $\text{CF}_4 + \text{O}_2$ |
| Adhesion to silicon dioxide | Excellent |
| Biocompatibility | Nonirritating to skin, no adverse effect on rabbits and mice, only mild inflammatory reaction when implanted |

Table 3.1: Typical material properties of PDMS [20]

3.1.2 Conductive materials

When producing stretchable circuits, not only is the substrate required to be stretchable, but also the conductive materials must allow the entire structure to deform. As such, two kinds of material are here described: PDMS-based conductive composites and liquid metal. The composites are the result of mixing PDMS with conductive particles, before cured, in order to make it conductive while still maintaining its ideal mechanical properties for biosensing. Compared with metallic conductors, conductive polymer composites have the advantages of ease of shaping, low density and wide range of electrical conductivities as well as corrosion resistance [30]. These soft material conductors have two distinct functions in the field of soft sensing: the sensing function itself and the conveying of electrical information in the circuit (interconnects). At the end of this section, a brief summary about the suitability (or not) of each material for such functions is presented.

3.1.3 zPMDS

zPDMS is, in this thesis, the designation of an anisotropically conductive PDMS composite, result of the blend between PDMS and silver-coated nickel (Ag-Ni) microparticles of $15\ \mu\text{m}$ diameter [26]. The name derives from the characteristic that the material films have of only conducting along the direction of their thickness (z-axis)(3.2).

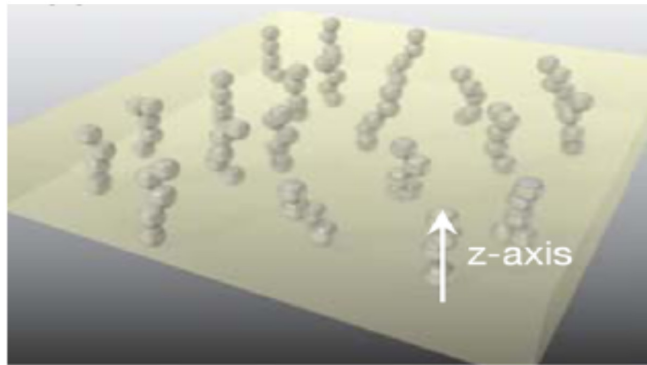


Figure 3.2: PDMS embedded with an array of vertically aligned columns of Ag-Ni that support conductivity only through the thickness of the film (z-axis) [21].

Ag-Ni particles are not only conductive, but also magnetic and, as such, form

vertically aligned columns if a vertical magnetic field is applied during the curing process. The fabrication of zPDMS films, therefore, consists in the following steps:

- homogeneous mixing of PDMS with Ag-Ni particles;
- deposition of the patterned film;
- placement of the sample on top of a flat magnet;
- curing at 180°C for 8 minutes.

The resistivity of the material is influenced by the filler (Ag-Ni) concentration, film thickness and area [26]. States that for a concentration of 20 wt%, the electrical resistance is low enough (0,6 Ω for an area of 9mm² and a thickness of 90 μ m) to support basic circuit and sensing functionality. The concentration chosen in this project for the developed circuit is 30 wt% [27].

The usage of zPDMS, however, only makes sense when combined with an isotropic conductor: in this work, for instance, zPDMS is used as a sensing component with a layer of liquid metal above, to convey the information gathered by zPDMS. This anisotropic characteristic, though, may be useful to avoid shortening between traces of liquid metal, and the fact that the concentration required for anisotropic conductors is considerably lower than for isotropic ones makes this kind of material easier to mix and pattern: when using the same particles of Ag-Ni to produce an isotropic conductor, the percolation threshold (minimum concentration to become conductive) is around 80 wt% [27].

3.1.4 AgPDMS

AgPDMS has previously been reported to be conductive at 21% (or 69 wt%) for pressure sensor applications and 83 wt% for droplet detection. SEM images were taken to observe the Ag concentration on the microchannel sidewalls as well as surface roughness. Figures 3.3(a) and (b) show 69 wt% Ag and 85 wt% Ag concentrations, respectively. These images shows the material composition of the bottom of the device and the sidewall of the channel. Since heavier elements provide a higher intensity signal, the bright dots represent Ag particles, and the remaining

grey structure represents the carbon-dominant PDMS. The density of Ag is significantly higher in figure 3.3(b), which resulted in a much higher conductivity of the AgPDMS electrode.

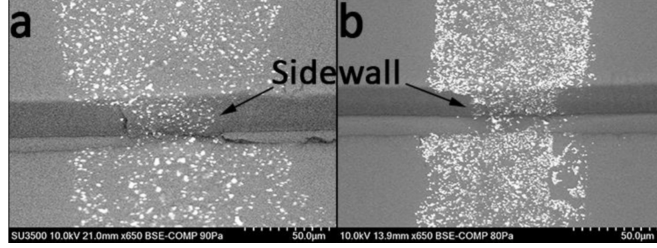


Figure 3.3: SEM images showing AgPDMS electrodes. (a) Device bottom and sidewall with 69 wt% Ag particles. (b) Device bottom and sidewall with 85 wt% Ag particles [28].

Thin strips of AgPDMS of various Ag concentrations were fabricated with the same dimensions of the electrodes used in the microfluidic device to further optimize conductivity. The conductivity values at different Ag concentrations are summarized (3.4).

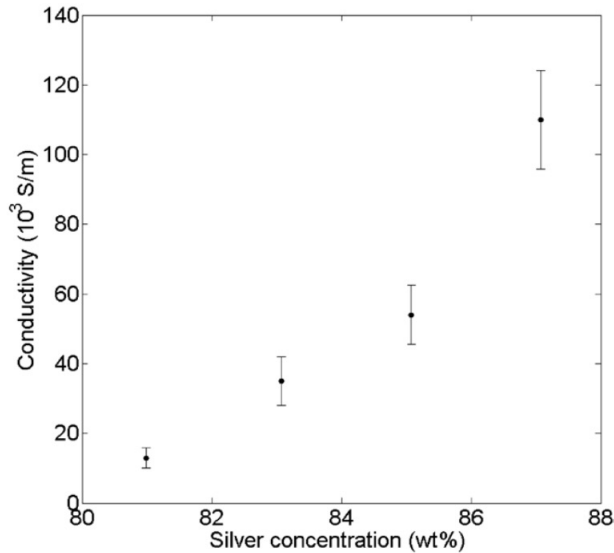


Figure 3.4: Conductivity of AgPDMS with varying Ag particle wt%. $n=3$ for each Ag concentration [28].

While concentrations greater than 81 wt% were found to have good conductivity

(>103 S m⁻¹), 85 wt% was found to have much higher conductivity while having the same ease of fabrication. AgPDMS with 87 wt% Ag started to become difficult to mix and have a clumpy, aky texture, compared to the more paste-like composition at lower concentrations. Therefore, our AgPDMS electrodes were fabricated using 85 wt% Ag (2.13) [28].

3.1.5 Silver Epoxy

Silver Epoxy Paste is a one component system designed as a conductive thermosetting silver preparation for screen printing applications [8]. Its composition is unique, providing high electrical and thermal conductivity with excellent bond strength after appropriate cure. Silver Epoxy Paste is used to advantage in place of lead-tin solders to avoid flux contamination or exposure to excessive temperature and for process simplification by screening on contacts [8].

Silver Epoxy Paste forms ohmic bonds with semiconductors if the surface of the semiconductor is metallized, or if the surface is highly “doped” and lapped. The product finds extensive use in bonding semiconductor chips, integrated monolithic circuits, diodes, transistors and other components in thin film and thick film hybrid microelectronic circuits. It bonds to glass, mica, plastic, graphite, quartz and other materials as well [8].

FEATURES

- One component system
- Excellent screening characteristics
- Develops high bond strength
- Low contact resistance
- Very low thermal stress
- Low thermal impedance
- Temperature -65 ° to +250 °C

3.1.6 Liquid metal

The designation of liquid metals is attributed to the class of metals or metal alloys that remain at a liquid state at room temperature. The integration of such materials in soft electronics is of great interest due to their superior conductivity, compared to other soft conductors like conductive composites, and ability to flow within elastomer patterned microchannels, guaranteeing a conductive path even under deformed conditions. The most traditionally used liquid metal is mercury but, due to its high toxicity, its use has been avoided; gallium alloys represent a safer alternative (3.5), being less toxic [11].



Figure 3.5: Conductivity test with liquid metal on the resistors path

A widely used liquid metal is the eutectic gallium-indium alloy (eGaIn) [17] and it is the one used throughout this project. eGaIn is an expensive material but easy to produce in lab by alloying both metals: to do so, gallium and indium must be weighted in the correct proportion (75,5 % and 24,5 %, respectively) and melted at 195°C. Similarly to rigid metals, eGaIn has a very low resistivity ($29 \times 10^{-8} \Omega\text{m}$) and its low viscosity allows it to be patterned into soft electronic systems with laser ablation [25], roller deposition [27], freeze casting [19], injection [17] and spray deposition [27] techniques. As such, liquid metals are a great material to form interconnects for soft stretchable sensors; as for the sensing function itself, however, they cannot be in direct contact with the skin due to their liquid form (liquid metals must be involved by the substrate, so they don't leak).

3.2 Equipment

A quick overview of the main equipment utilized throughout the work is in this section.

3.2.1 Laser cutter

The laser cutter used is the *VLS3.50 Desktop*, by *Universal Laser Systems*. Equipped with a CO_2 laser source, its power ranges from 10 to 50 watts (3.6).



Figure 3.6: Laser cutter

A laser is a device that emits a beam of coherent light through an optical amplification process. There are many types of lasers including gas lasers, fiber lasers, solid state lasers, dye lasers, diode lasers and excimer lasers. All of these laser types share a basic set of components [7].

Laser cutting is the complete removal and separation of material from the top surface to the bottom surface along a designated path. Laser cutting can be performed on a single layer material or multi-layer material [7].

When cutting multi-layer material, the laser beam can be precisely controlled to cut through the top layer without cutting through the other layers of the material (3.7).

Material thickness and density are important factors to consider when laser cutting. Cutting through thin material requires less laser energy than cutting the same material in a thicker form [7]. Lower density material typically requires less laser energy. However, increasing laser power level generally improves laser cutting speed [7].

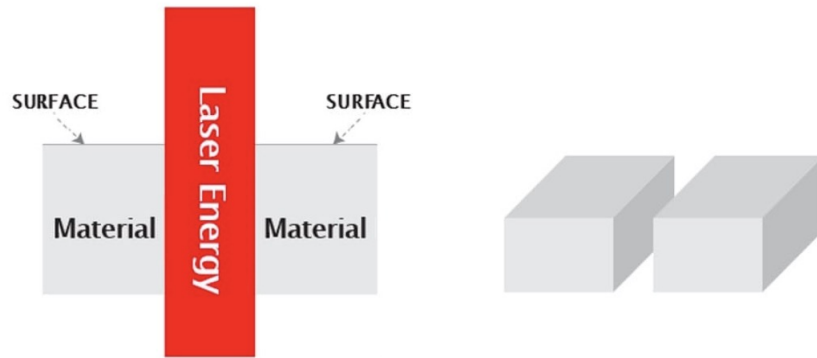


Figure 3.7: Example of laser cutting [7].

In general, CO_2 lasers with 10.6 micron wavelength are primarily used for cutting non-metal materials. CO_2 and fiber lasers are both used for cutting metals. However, as a rule, cutting metals requires substantially higher power levels than non-metal materials [7].

3.2.2 T962C Reflow oven

The oven used is the *T962C Reflow oven*, works automatically by micro-computer control and its rated power can reach 2500 W (3.8).



Figure 3.8: T962C Reflow oven

MAIN FEATURES

1. Have big infrared soldering max area.
2. Many temperature wave choice.
3. Special heat up and temperature equalization with all design.
4. Humanized science and technology exquisite article.
5. Perfect function choice.

3.2.3 Thinky ARE-250 mixer

The *Thinky ARE-250* mixing and degassing machine is an industrial non-contact “planetary” mixer for all engineering compounds (3.9). It mixes, disperses and degasses your materials in seconds to minutes, in a sealed or lidless container such as a jar, beaker, syringe tube or cartridge [4]. The non-contact mixing principle makes it possible to formulate compounds from very small amounts such as 0.5 ml to large production scales [4].

It makes possible for the processes of mixing and bubble removal to be carried out simultaneously [4]. It is a conditioning mixer that it can be used for the mixing and/or bubble removal of not only epoxy but also silicones, conductive pastes, medicines, chemical materials, etc.



Figure 3.9: Thinky ARE-250

The *Thinky ARE-250* mixer is a lightweight benchtop model, which can hold up to 310g of material [4]. The Multi-Step mixing feature allows you to program 5 different sets of mixing and degassing conditions (time and speed per mode) in a single batch cycle. Precise control of the process makes it possible not only to improve formulation quality, but also to eliminate human errors or operator skills throughout the process. It is also effective in controlling shear, so as not to damage the materials [4].

TECHNICAL PARAMETERS

- Dimensions: 390x300x300mm
- Weight: 22Kg
- Power requirements: 230V +/- 10% 50Hz
- Minimum material capacity: 0.5g
- Maximum capacity: 310g
- Timer: Set up to 30 minutes, 1 second increments
- Programming: Mixing and/or degassing mode, multi-Step mixing, speed changer
- Memory: 5 memory slots are available for different 5 batch cycles. Programmed mixing procedure can be recalled in a second

3.2.4 ZUA 2000 Universal Applicator

With a range from 0 μm to 3000 μm , the *ZUA 2000 Universal Applicator*, by *Zehntner GmbH Testing Instruments*, was used throughout this work to produce thin uniform elastomer films (3.10).

HANDLING

1. Only use on solid substrates such as vacuum plates, glass plates, test panels, test charts



Figure 3.10: ZUA 2000 Universal Applicator [9].

2. Adjust the applicator to the desired gap height and place it on the substrate to be coated
3. Pour the product to be tested in front of the applicator in drawing direction and apply with uniform speed of about 25 mm/s
4. Afterwards disassemble the applicator and clean it

| | |
|------------------------|---|
| Material | red, hard finish, solvent-resistant aluminium |
| Adjustable gap heights | 0 μm - 3'000 μm (0 mil - 118.11 mil) |
| Graduation/resolution | 5 μm (0.20 mil) |
| Tolerance | $\pm 10 \mu\text{m}$ (0.39 mil) |
| Standard film widths | 60 mm, 80 mm, 100 mm, 150 mm, 200 mm or 220 mm (2.36", 3.15", 3.94", 5.90", 7.90" or 8.70") |
| Weight | 229 g - 479 g (0.50 lbs - 1.06 lbs), depending on version |
| Warranty | 2 years |

Table 3.2: ZUA 2000 Universal Applicator technical specification [9].

Chapter 4

FABRICATION METHODS

In this chapter, some of the state of the art fabrication methods in stretchable electronics, that were also employed during the course of this work, are briefly summarized. Furthermore, the specific fabrication methods used to produce each parts of circuit displayed in dissertation are also explained.

4.1 Circuit's design on PCB

Before starting to discuss about the extensible electronics, a similar circuit in PCB was fabricated to test if the network of resistors and capacitors works correctly. To do this, the EAGLE program was used.

The main components of this circuit are:

- **MAX30003** (4.1): MAX30003 is a single-lead ECG monitoring IC which has built-in R-R detection and several other features that make it perfect for a wearable single-lead ECG application. Several new features on this chip make it ideal for wearable applications. First is the low power consumption - just 85 uW of power and can work from 1.1 V onwards. Also of interest is the fact that it can work with only two chest electrodes without the need for a third right-leg drive (DRL) electrode.

The best feature of this chip though is the built-in R-R detection algorithm which can measure the time between successive peaks of the QRS complex of the ECG. This means that heart-computation comes right out of the box without any microcontroller-side code requirement.

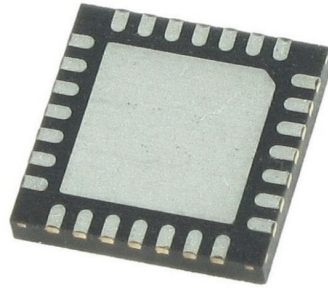


Figure 4.1: MAX30003's chip

- **TXB0108PWR** (Logic level converter) (4.2): This 8-bit noninverting translator uses two separate configurable power-supply rails. When the output-enable (OE) input is low, all outputs are placed in the high-impedance state. The TXB0108 is designed so that the OE input circuit is supplied by VCCA. This device is fully specified for partial-power-down applications using Ioff. The Ioff circuitry disables the outputs, preventing damaging current backflow through the device when it is powered down. To ensure the high-impedance state during power-up or power-down, OE should be tied to GND through a pulldown resistor; the minimum value of the resistor is determined by the current-sourcing capability of the driver.

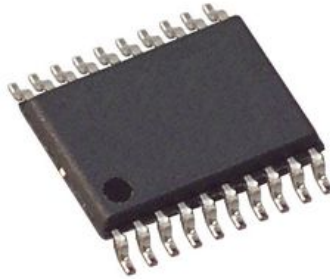


Figure 4.2: Logic level converter

- **AP2112K-1.8TRG1** (Voltage Regulator): The AP2112 is CMOS process low dropout linear regulator with enable function, the regulator delivers a guaranteed 600mA (min.) continuous load current. The AP2112 provides 1.2V, 1.8V, 2.5V, 2.6V, 2.8V and 3.3V regulated output, and provides excellent output accuracy $\pm 1.5\%$, also provides an excellent load

regulation, line regulation and excellent load transient performance due to very fast loop response. The AP2112 has built-in auto discharge function.

The scheme below shows the whole circuit divided into main components (4.3). The upper left part shows the MAX30003 with its electrode outputs (JP3), the upper right part shows the voltage regulator that limits the voltage from 3.7 V to 1.8 V. In the lower right corner there is the logic converter, placed between the MAX30003 and the connectors (bottom left), which takes care of the data connection between the various components of the circuit.

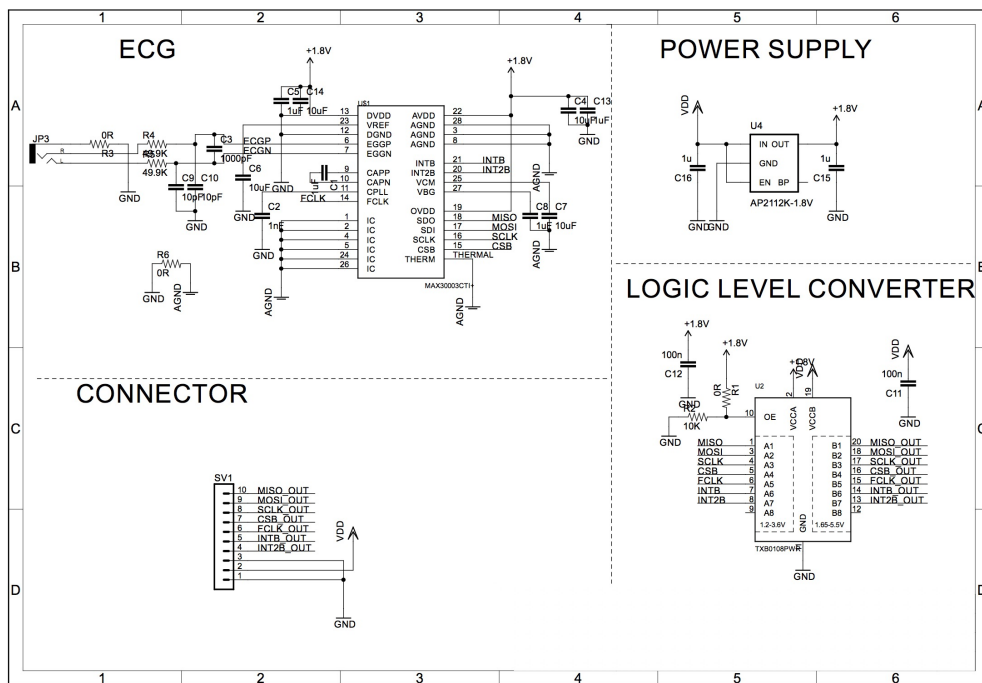


Figure 4.3: Circuit’s schematic.

Once the circuit has been designed manually, proceed with bringing everything on eagle (4.4a), useful then to print the circuit on PCB (4.4b).

After the production of the circuit it was necessary to connect the PCB with another programmable logic board (*Arduino UNO*) (4.1), program it with a dedicated software, and connect everything to the computer, where to read the data there is a program (*Healthy Pi*) with is possible to see the waves of the electrocardiogram. In the table below there are all the connections between *Arduino UNO* and PCB

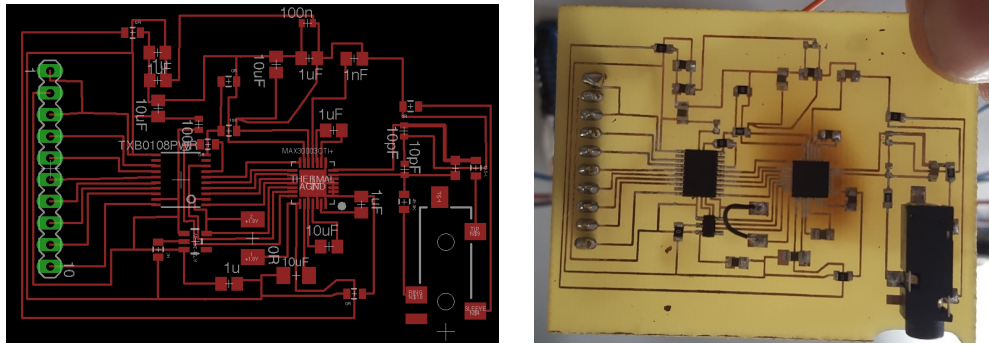


Figure 4.4: Circuit on Eagle on the left (a) and PCB on the right (b).

with their functions.

| MAX30003 pin label | Arduino Connection | Pin Function |
|--------------------|--------------------|------------------------------------|
| MISO | D12 | Slave out |
| MOSI | D11 | Slave in |
| SCK | D13 | Serial clock |
| CS0 | D7 | Slave select |
| FCLK | D6 | External clock(32KHz) |
| INT1 | NC | Interrupt |
| INT2 | NC | Interrupt |
| 3V3 | Supply | Board which supports 3.3V and 1.8V |
| VCC | Supply 5V | 5V |
| GND | Gnd | |

Table 4.1: Connections between PCB and *Arduino UNO*.

Programming: After configuration I had to program the PCB with *ARDUINO*'s code to test the effective operation of the circuit (Appendix A).

The following chapter contain the results of the electrocardiograms with three different types of electrodes:

1. **Wet-contact electrode**
2. **zPMDS electrodes**
3. **AgPDMS electrodes**

4.2 Circuit’s design on flexible PCB

To export the circuit on the flexible PCB, has been redesigned some parts of the circuit because was necessary the bluetooth module to send the data to the PC. To do this has been chosen *CYBLE-022001-00* module (4.5) but to program this chip has been used another program as *PSoC Creator*. To check the programming code has been inserted it in *CY8CKIT-042-BLE-A* board, that has integrated bluetooth; it’s appropriate to specify that the programming code of the CPU in the *CY8CKIT-042-BLE-A* and the *CYBLE-022001-00* are the same.



Figure 4.5: CYBLE-022001-00 module

The idea initially was to design the entire circuit on a single layer of PDMS like the following figure shows:

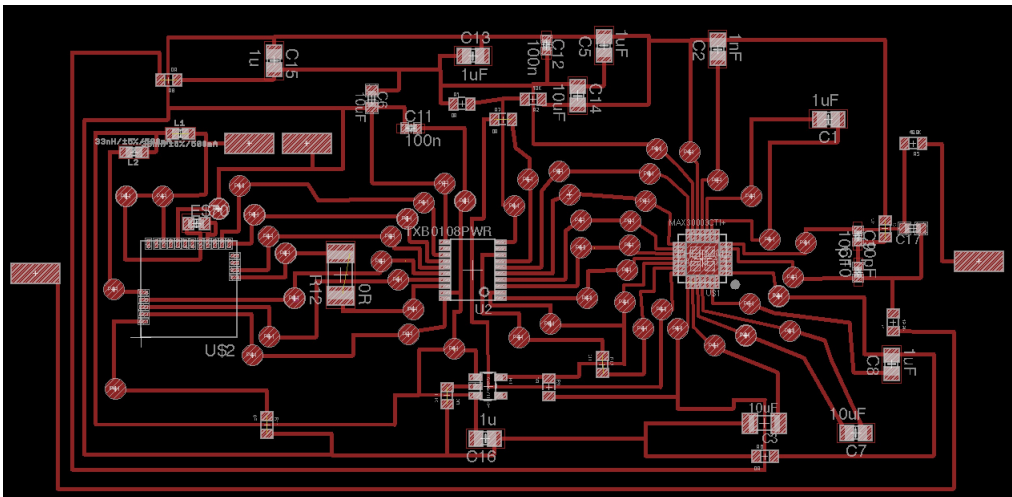


Figure 4.6: Circuit with one layer: on the left we have *CYBLE-022001-00* module, in the centre *TXB0108PWR* (Logic level converter) and on the right *MAX30003*.

To get to the realization of this circuit have been implemented some specific procedures, the same ones that implement for the electrode manufacture with AgPDMS

electrodes (2.12) so: stencil, PDMS and 85 wt% of AgPDMS, with the remaining 15% a mix of *SYLGARD* (silicone elastomer curing agent) and PDMS, respectively 1 to 10.

As we can see from the project there are four rectangles, two side and two in the central area: the first two are used to connect the electrodes and are placed in that position to pick up the signal coming from the heartbeat (4.7), the other two are used to connect the battery.



Figure 4.7: Electrodes's position

Another detail to note are the circular pads that surround the three chips: those circular pads means the circuit/chips connection, because the basic idea was that the chips didn't have to be connected directly on the circuit but on copper coated kapton sheets (flexible PCBs), in a way that makes the circuit flexible and extensible as possible.

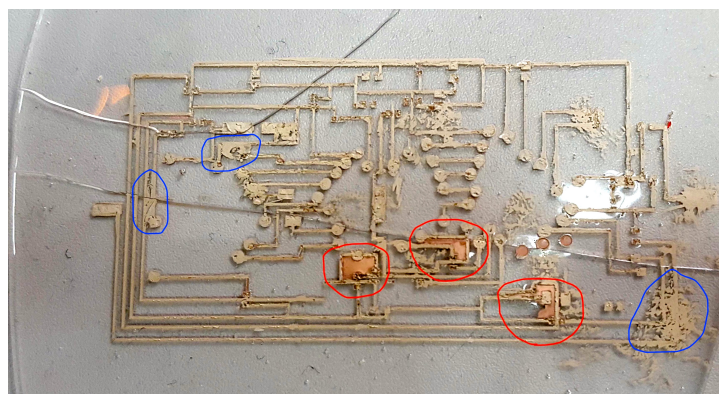


Figure 4.8: Circuit with one layer (flexible): the problems are represented in red circles and in the blue ones there are problems related to damage on the circuit lines.

But with this method have been problems, because the lines of the circuit were too close to each other and therefore, when has been removed the stencil, in some places it remained there because the force needed to remove it was not small and so it was very easy to break it. Then it was impossible to remove the pieces left because it was very easy to damage the lines's circuit near them (4.8). Has been redesigned the circuit on several levels, in other words two layers (4.9). This solution, in addition to solving the above problem, also has the benefit of being able to eliminate many of the resistors that have the bridge task (0 ohm) to connect segments of the same line. So, in this way, the circuit became easier to produce maintaining anyway flexibility and extensibility.

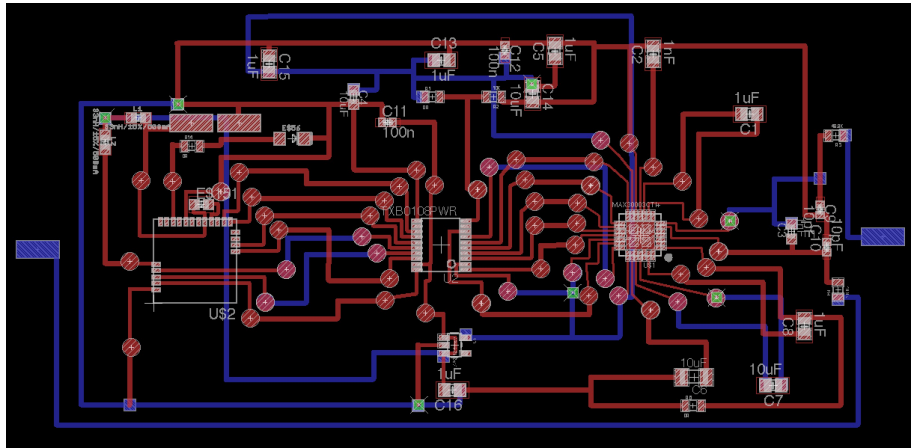


Figure 4.9: Circuit with two layer: the blue ones is the first layer the red ones is the second.

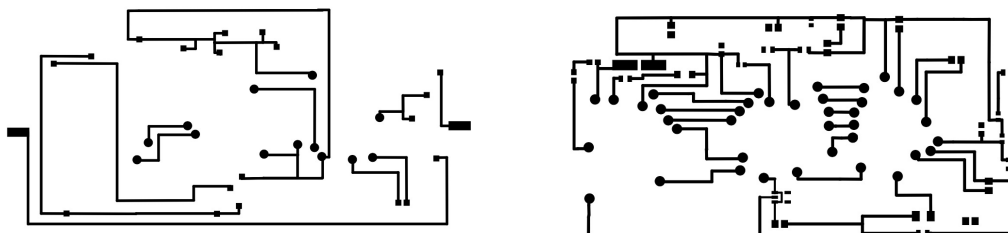


Figure 4.10: Separate circuit layers

As you can see from the CAD image some components of the circuit are connected on the first layer (C7 and the electrodes), others on the second (chips), others

with a pad on the first layer and the other one on the second. Having said that to get around this problem, have been performed with the laser some holes in correspondence to those pads or circular pads where the first and second layers meet, in order to have the connection of the first layer also on the surface, where it was necessary. The pads of the electrodes are also included.

Before starting to illustrate the manufacturing process of this circuit it is opportune to specify that to match exactly the chips to the circuit, it was necessary to implement the mirroring of the circuit, because the chips must be turned updown and fixed.

Below there are the steps for making the two layers circuit:

1. Before describing the images in (4.11), it should be remembered that the circuit is made on a glass plate on which a thin layer of PDMS (200 μm) by *ZUA 2000 Universal Applicator* is spread and placed into the oven for 30 minutes at 150 degrees to solidify it.

After that, has been applied a layer of stencil paper on the layer of PDMS, so as to be able to carry out on it, by laser, the trace of the first layer of the circuit (4.11 left). Then has been filled these tracks with AgPDMS (85 wt%) (4.11 right), finally removed the stencil paper and put it into the oven for 40 minutes at 150 degrees.

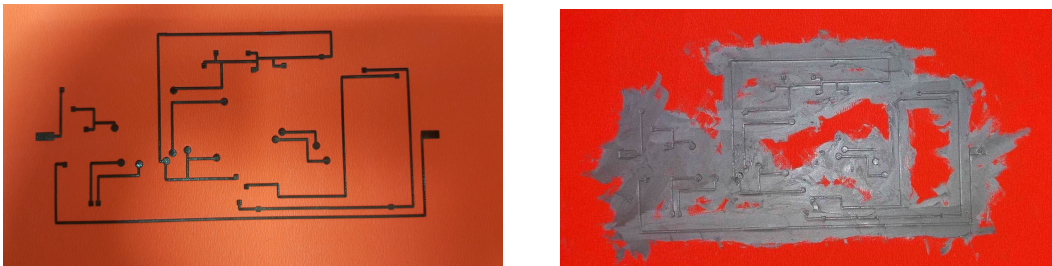


Figure 4.11: Fabbriation of first layer: stencil paper cut with laser (left), AgPDMS on the first layer trace (right).

2. In the next step was necessary to remove the previous circuit from the oven (4.12 left), place on top of it another layer of PDMS (200 μm) and place again in the oven for another 30 minutes at 150 degrees. Once outside, has been

placed another layer of stencil paper above the circuit and cut the traces of the second layer of the circuit by laser (4.12 right).

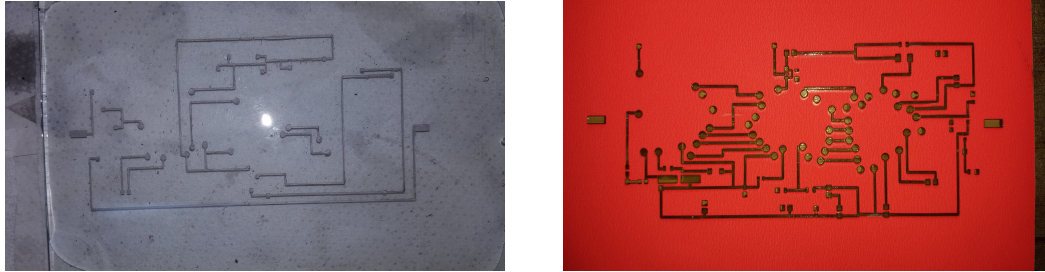


Figure 4.12: Result of the first layer (left), preparation of the second layer (right).

3. In the next step have been made more holes in correspondences of the points where the circuit of the first layer must be in contact with the second, for a correct operation (4.13 left). After checking with the multimeter if there was or not the connection between the two layers, has been spread the AgPDMS over the entire surface again, being careful to fill correctly all the holes (4.13 right).

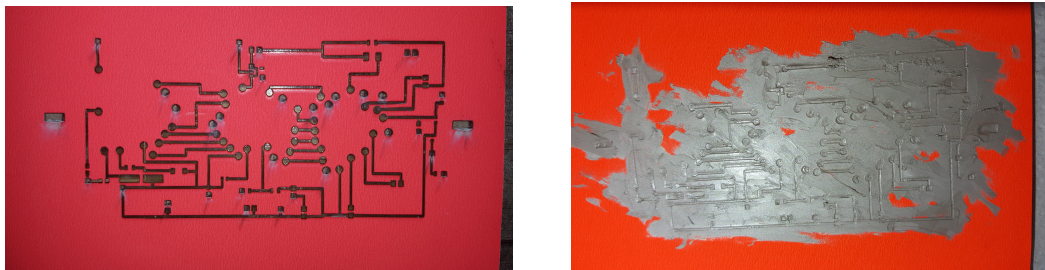


Figure 4.13: Holes in the points where must to be contact between two layers (left), AgPDMS on the second layer trace (right).

4. For the last step of the manufacture has been gently removed the stencil layer and put the whole circuit into the oven for 40 minutes at 150 degrees. The final result is shown in the figure below (4.14).

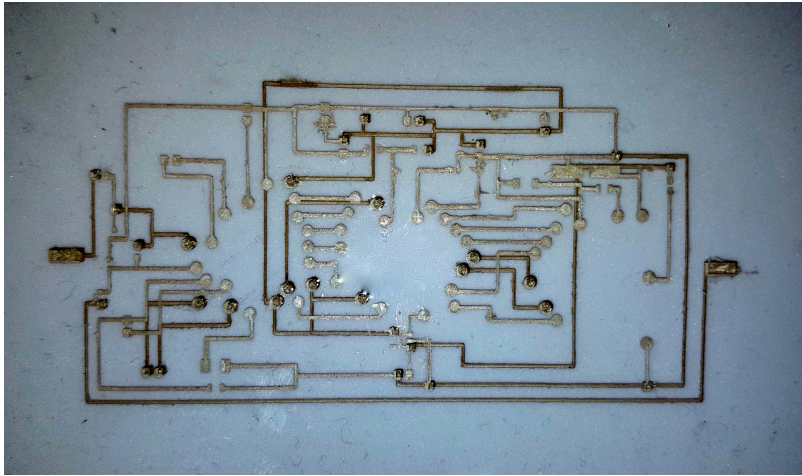


Figure 4.14: Final circuit with two layers

4.3 Chips connection

The next step, once the base of the circuit was built, is the integration of the chips on the circuit. However, this process required two other intermediate steps, namely: fixing the chip on the copper paper and fixing it on the circuit.

The first of the two for fixing required chemical processes and welding, the latter required the use of zPDMS and a lot of precision.

4.3.1 Fixing of the chips

To weld the chips on the copper coated kapton sheet (4.15) it was necessary to have a printer, in my case have been used the *Xerox ColorQube 8580*, and some chemical agents such as caustic soda and ferric chloride.

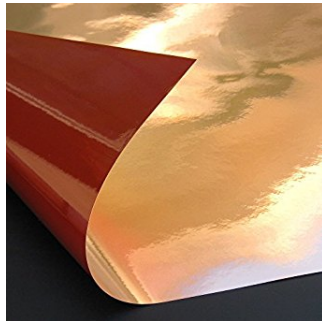


Figure 4.15: Copper coated kapton sheet.

The procedure for producing flexible PCB is as follows:

1. Export the chip CAD from Eagle to pdf (4.16).
2. Print the chip and cover the printed chip with a copper coated kapton sheet.
3. Reprint the chip on the copper coated kapton sheet.
4. Place the copper coated kapton sheet under UV light for 20 minutes.
5. Immerse it in the caustic soda until the photosensitive film is eliminated.
6. Immerse it in the ferric chloride, about two hours, to remove the copper not located on the printed traces.
7. Spread only on the circular pads the liquid metal, to improve the conduction with the rest of the circuit (4.17 left).
8. Solder the chip (4.17 right).

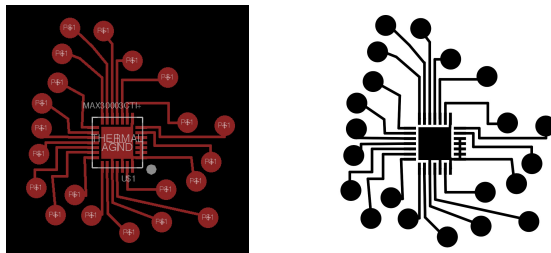


Figure 4.16: Chip from CAD to PDF.

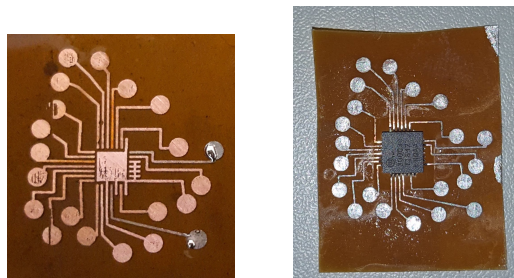


Figure 4.17: Flexible PCB and welding of the chip.

The figure below shows all three chips on flexible PCBs (4.18).

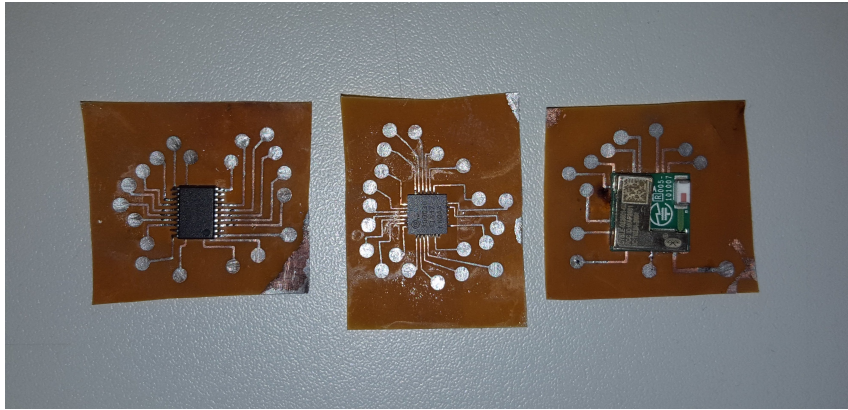


Figure 4.18: Chips on the flexible PCBs: on the left the *TXB0108PWR* in the centre the *MAX30003* on the right the *CYBLE-022001-00*.

4.3.2 Fixing of the copper coated kapton sheet

To understand how to connect the flexible PCB to the final circuit (4.14) has been used the zPDMS (3.2), which is easy to implement on the surface of the circuit, since it only leads to contact points and acts as glue.

To test the zPDMS has been examined only one of the three previously mentioned PCBs, the MAX30003 and then built a CAD circuit around it adjacent to its contact points (circular pads) (4.19, left). In this way it was possible, through a multimeter, to check if there was a connection between the flexible PCB and the circular pads placed at the end of the CAD through the central ones.

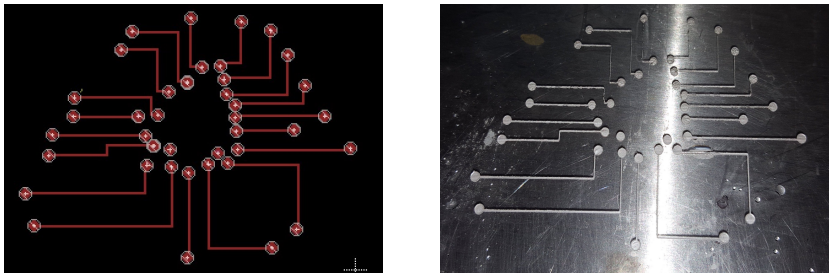


Figure 4.19: CAD circuit to test the conductivity between flexible PCB and circular pads (left), circuit with PDMS and AgPDMS after oven (right).

After the production of the circuit in figure (4.19, right), using the same technique of the final circuit (4.14) and the electrodes with AgPDMS (2.13), applying the *ZUA 2000 Universal Applicator*, has been spread a layer of zPDMS with a thickness of

200 μm on its surface (4.20).

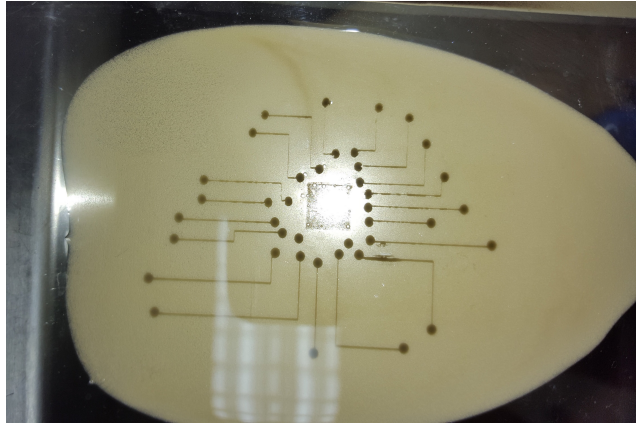


Figure 4.20: zPDMS on top of the test circuit.

The next step will be to fix the flexible PCB on the zPDMS layer before inserting the circuit in the oven for solidification (4.21).

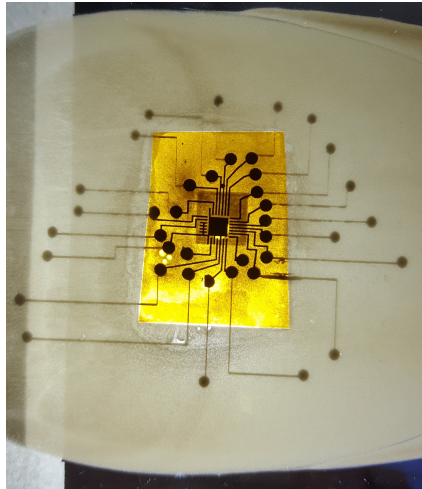


Figure 4.21: PCB on the zPDMS in correspondance of the circular pads (top view).

This is a very delicate and important step because, given the manual work and the small size of the circuit, was very easy to make some mistakes: the most frequent was to exert a non homogeneous pressure that involved a different distribution of the zPDMS, causing the loss of the latter in some circular pads (4.22, left).

Said that, being very careful to the pressure to apply, has been inserted the test into

the oven for 30 minutes at 150 degrees.

The results are visible in the figures below.

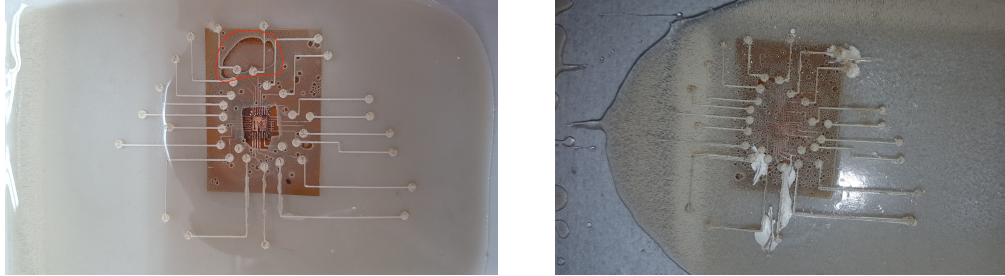


Figure 4.22: On the left the test with mistake for the pressure in the red circle, on the right the correct circuit (bottom view).

4.4 Resistors and capacitors connection

The last step to complete the construction was to understand how to connect capacitors and resistors, so has been applied and tested two different methods: zPDMS and Silver Epoxy.

This procedure has proved to be less complicated than the chips because the positioning of capacitors and resistors is much more immediate, in fact has been sufficient to place the latter directly on the final circuit at their predetermined points.

4.4.1 Test with Silver Epoxy

To test the actual functionality of the Silver Epoxy has been built a test circuit, with PDMS and AgPMDS. (4.23, left).

As you can see, there are segments of AgPMDS with the end of the circular pads, for measurement by the multimeter, and in the middle rectangular pads where instead will be a connection by positioning the resistors.

After removing the test circuit from the oven (for the solidification of the Ag-PDMS) and allowed to cool, has been placed the Silver Epoxy on the rectangular pads, placed $0\ \Omega$ resistors, and placed the circuit test into the oven for 20 minutes at 150 degrees for solidification.

The final result is illustrated in the figure (4.23, right).

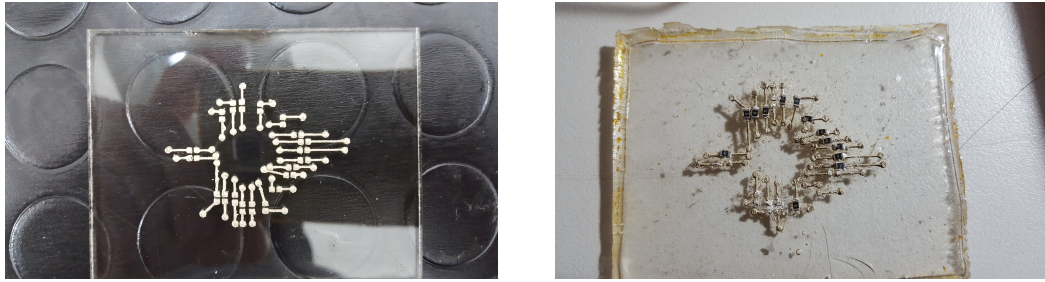


Figure 4.23: Silver Epoxy test.

4.4.2 Test with zPDMS

For this test, it is necessary to specify that has been placed the liquid metal at the extremity of each capacitor and resistor, before positioning them on the circuit, to facilitate the passage of current. But for this test, unlike the previous one, have been inserted resistors with a value of 560 ohms.



Figure 4.24: Final test circuit with resistors on zPDMS.

In this case, the placing of the components with the zPDMS, turns out to be much simpler, because the latter is more viscous than the Silver Epoxy and so more resistant to small accidental variations due to manual movement.

Taking into consideration the previously used circuit, has been distributed the zPDMS only where it was needed, I mean, on the rectangular pads. After 30 minutes in the oven the result is in the following figure (4.24).

Chapter 5

RESULTS

Despite the acquisition of know-how on the manufacture of stretchable circuits for bio-monitoring patches, the main objective of this thesis is also to compare various types of electrodes to each other in terms of functionality, that is, the fidelity of the signal reproduced of the acquired heart rate, as well as the signal quality for each of them when applied over the skin, compared to commercial electrodes (wet-contact electrodes).

To do this, have been considered two types of electrodes available, namely the zPDMS and AgPDMS electrodes, as well as the wet-contact electrodes as reference. Therefore a heart rate signal acquisition system was applied (*Healthy Pi*). Subsequently, the results of the tests performed for the complete construction of the two-layer circuit, components and chips, will be analyzed.

5.1 ECG with no flexible PCB

This section will compare the results of the ECGs of the various electrodes starting from the wet-contact ones. To test the electrodes has been configured the *CY8CKIT-042-BLE-A* board as in the figure (5.1); it's appropriate to specify that all the results are in bluetooth mode.

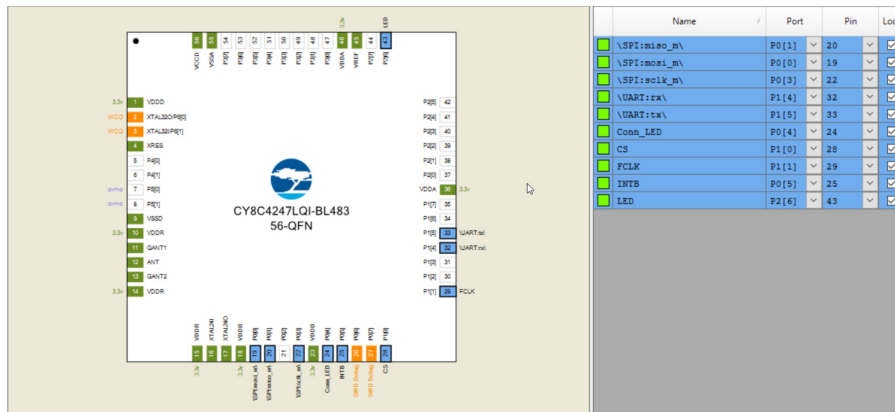


Figure 5.1: CY8CKIT-042-BLE-A chip configuration

5.1.1 Wet-contact electrodes

After configuring the chip and downloading the program on the board, have been obtained the first results:



Figure 5.2: First results with bluetooth mode and wet-contact electrodes.

As you can see the results aren't so perfect because the acquired signal is full of noise due to the length of the electrode and USB cables used for the connections and for the considerable amount of electronic equipment present inside the laboratory, but nevertheless are very similar to the image 1.6, taken as a reference for these tests. In addition to the ECG waveform, another important factor to consider is the cardiac frequency, which is also excellent because the average of the results obtained (about 78.5 BPM) falls within the range of the cardiac frequency of an adult that typically goes from 60 to 90 BPM. Further checks will be examined in the following paragraphs.

Finally, it is fair to specify that, in the upper right and bottom left figures, there are two PQRST waves nearby, but it is only a causality due to the movement of the cursor that updates the ECG wave.

5.1.2 zPDMS electrodes

After the verification the actual functioning of the PCB, through the commercial electrodes, has been verified the trend of the heart rate with the zPDMS electrodes (5.3), with the same settings.

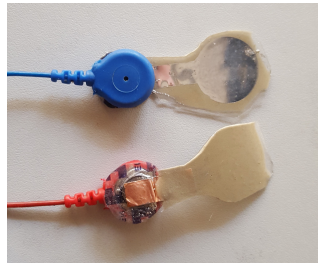


Figure 5.3: zPDMS electrodes for measurement

Some results are shown in the following figures.

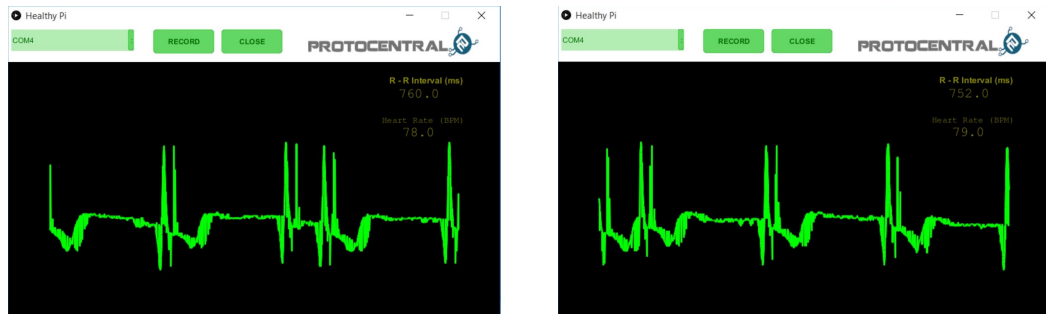


Figure 5.4: First results with zPDMS electrodes.

As it is easy to see the results obtained, aren't absolutely in line with those obtained with the wet-contact electrodes, for this reason they will not be taken into account for the final project.

5.1.3 AgPDMS electrodes

The last test to perform has been with AgPDMS electrodes (2.13). The results of the ECG are shown in the following figures.



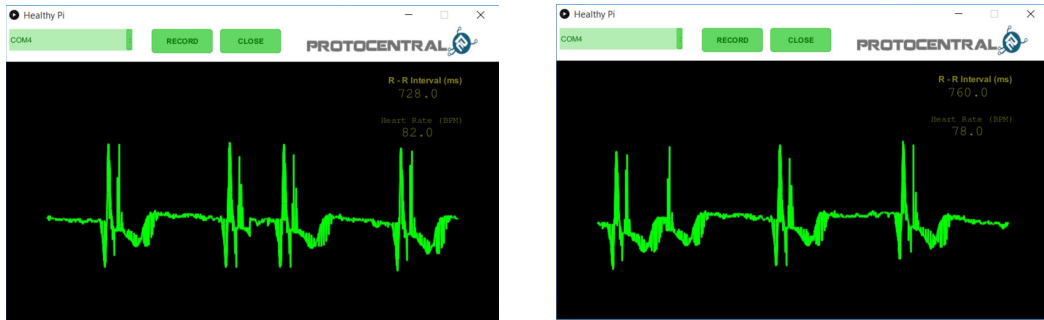


Figure 5.5: First results with AgPDMS electrodes.

Given the results it was easily possible to note the similarity with those obtained by means of the wet-contact electrodes, both for the shape of the ECG wave and for the average heart rate (about 79 BPM). The problem of excessive signal noise remained due to the same circumstances where it was also performed the previous tests. For this reason has been chosen to take the AgPDMS for the completion of the final circuit.

5.2 BPM comparison

Given the choice of electrodes, to see their actual reliability, has been decided to compare the cardiac frequency of the latter with another instrument for measuring heart rate, ie a smartphone with an integrated heart rate sensor. To have a large comparison has been examined the heart rate in two different situations: standing and sitting.

The results obtained are summarized in the following tables:

| STANDING | | | | | | | | |
|------------------------|----|----|----|----|----|----|----|------|
| Samples | 1 | 2 | 3 | 4 | 5 | 6 | 7 | AV |
| Wet-contact electrodes | 71 | 74 | 74 | 73 | 73 | 72 | 73 | 72.8 |
| Smartphone | 72 | 75 | 74 | 73 | 75 | 71 | 74 | 73.4 |
| AgPDMS electrodes | 78 | 79 | 80 | 78 | 77 | 78 | 76 | 78 |

Table 5.1: Standing comparison table

| SITTING | | | | | | | |
|------------------------|----|----|----|----|----|----|------|
| Samples | 1 | 2 | 3 | 4 | 5 | 6 | AV |
| Wet-contact electrodes | 66 | 66 | 67 | 67 | 66 | 68 | 66.6 |
| Smartphone | 68 | 66 | 66 | 65 | 68 | 68 | 66.8 |
| AgPDMS electrodes | 69 | 68 | 69 | 69 | 67 | 68 | 68.3 |

Table 5.2: Sitting comparison table

From the tables above it was possible to notice how the average BPM are very similar to each other, especially in the seated condition.

5.3 Stretchable circuit

After analyzing and comparing the heart rates of electrodes and sensors, it is necessary to analyze the results obtained by the two layers circuit. Being initially without components and chips, the first values to check are the correct connections of the network both on the same layer and between different layers (5.6). The following figure highlights some measurements between the various connections in the circuit.

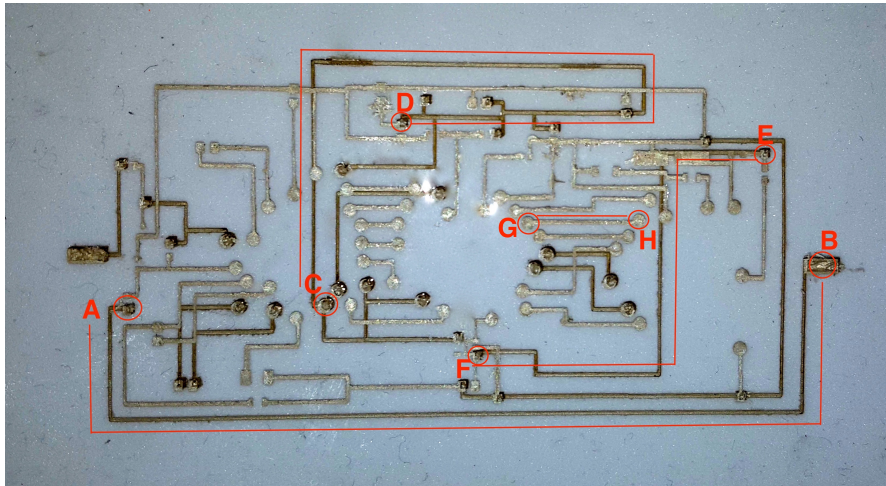


Figure 5.6: Final circuit measurements.

In the picture you wanted to examine the paths and then the points that connect the two layers. As you can see some traces of the network are darker than others,

because they are part of the first layer. It's precisely the connection of these traces that is the first that must be checked because it was necessary to know immediately if the two layers are connected. Thus, the points circled in the picture (A,B,C,D,E,F) are some of the holes drilled in the figure (4.13, left), instead the points G and H are both belonging to the last layer. The ohmic values of the routes are shown in the table below.

| Segment | Value |
|---------------------------|--------------|
| A \longleftrightarrow B | 3 Ω |
| C \longleftrightarrow D | 2.4 Ω |
| E \longleftrightarrow F | 2.2 Ω |
| G \longleftrightarrow H | 1.5 Ω |

5.3.1 Chips connection

After the analysis of the circuit network, the next step to analyze is the connection obtained between the copper coated kapton sheet of the chip and the test circuit (4.22, right). In the figure below (5.7) just some of the connection points between the PCB and the circular pads on the outside are shown.

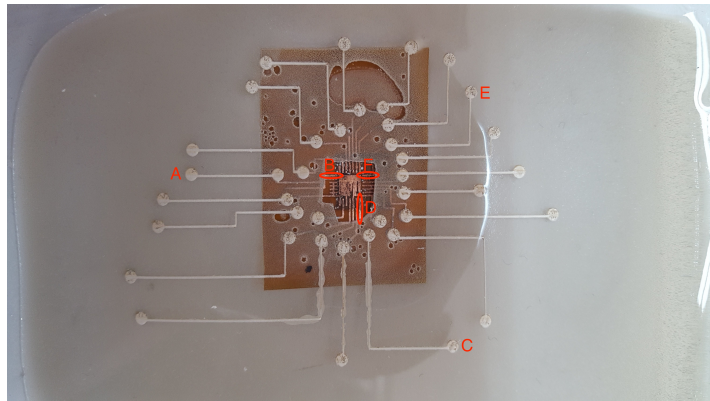


Figure 5.7: PCB - circuit measurements

In the table below there are the values of the paths taken into account.

| Segment | Value |
|---------------------------|--------------|
| A \longleftrightarrow B | 0.2 Ω |
| C \longleftrightarrow D | 0.3 Ω |
| E \longleftrightarrow F | 0.2 Ω |

5.3.2 Resistors and capacitors connection

The last step to examine before implementing everything on the final circuit, is the connection of resistors on the surface of the circuit (4.24). For this test have been used two different materials: Silver Epoxy and zPDMS. For the first the results were not satisfactory because the Silver Epoxy did not solidify, so there wasn't connection; the second one, however, has brought excellent results.

To check the measurement has been used a multimeter at the extreme points of the segments containing the resistors (560Ω). The following figure shows the segments analyzed.



Figure 5.8: Resistors measurements

In the table below there are the values of the resistors taken into account.

| Segment | Value |
|---------------------------|----------------|
| A \longleftrightarrow B | 560.1 Ω |
| C \longleftrightarrow D | 574.3 Ω |
| E \longleftrightarrow F | 574.6 Ω |
| G \longleftrightarrow H | 573.3 Ω |

From the table it is easy to notice that the values obtained are in accordance with the values of the resistors used. Moreover, the fixing of the resistors in their points is also an excellent result.

5.4 Final circuit

For the realization of the final circuit it was necessary to use:

- AgPDMS electrodes
- Two layers circuit network
- fixing of the chips with a layer of zPDMS
- fixing of the components with a layer of zPDMS

Even if there were four steps to perform, these must to be implemented together at the same time because the thin layer of zPDMS can be distributed only just one time being placed it in the oven (the introduction of another layer would not allowed the connection on the z axis between different columns).

But during the placement of the chips occurred an unexpected problem: the chips on the PCBs turned updown, were too thick and did not allow the direct contact of the circular pads on the PCBs with those of the circuit. To underline the fact that, could not be drill the circuit to fit the chips because doing so could damage the bottom layer.

Given this, the simplest solution is to fix on each circular pads the resistances of 0Ω on the vertical axis (5.9). Better solutions will be analyzed later.

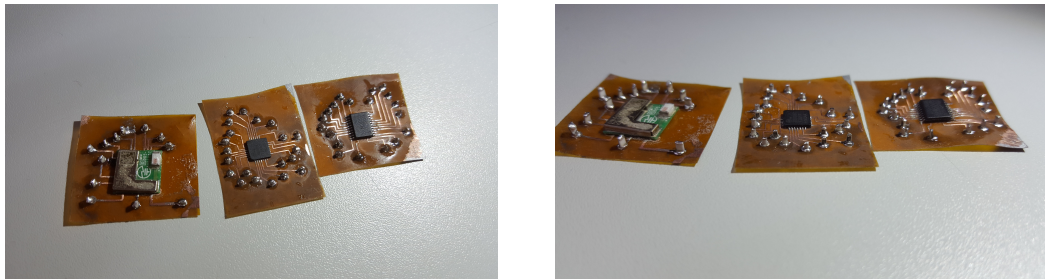


Figure 5.9: Connection with resistors.

The figure (5.10) shows the new way in which has been implemented the chips on the circuit.

Solved this problem it was possible to assemble all the components. Now, with this new arrangement of the chips, special attention should be given than the previous installation, because aligning the small side surface of the resistors is more difficult than the previous circular pads, due to the lack visibility and distance between the surfaces.

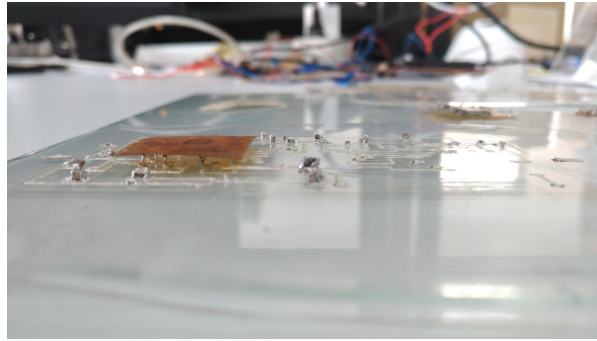


Figure 5.10: Chip placement.

Having said that, it is possible to proceed step by step to the realization of the final circuit. The following photos illustrate the complete circuit before introduction into the oven (5.11, 5.12).

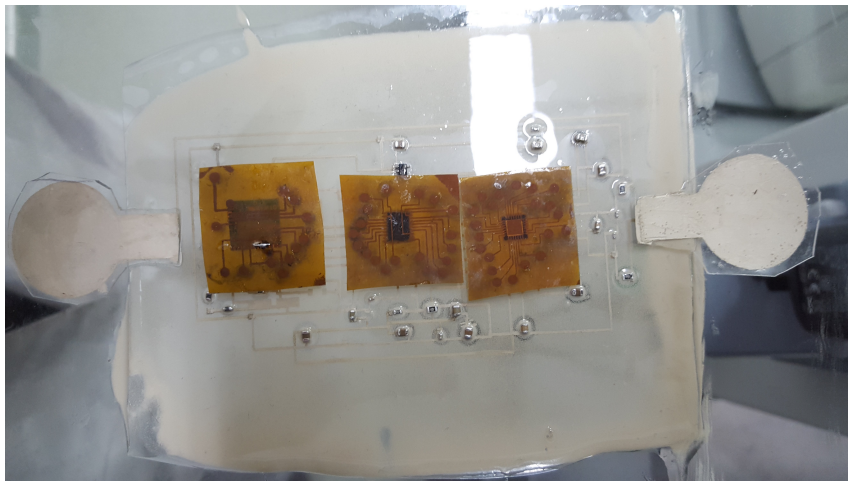


Figure 5.11: Complete circuit (top view).

Once all the elements have been positioned on the surface of the circuit, it was possible to insert it into the oven but, during this process, occurred an unexpected problem with the magnet. Being the biggest circuit than the previous tests, it was necessary to have a bigger magnet. This increase in size inevitably also causes an increase in power that affects the lines of the magnetic field, causing the displacement or rise of resistors and capacitors of smaller dimensions.

Given the problem, was attempted to resolve it by placing the circuit at a greater

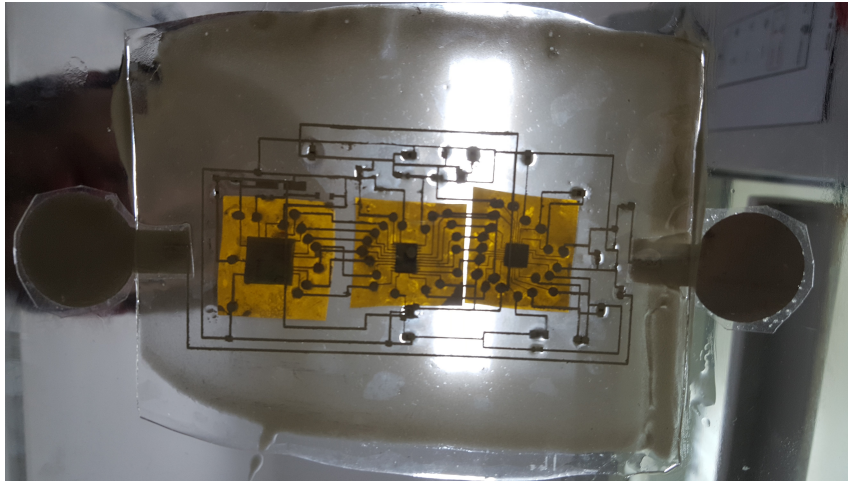


Figure 5.12: Complete circuit (bottom view).

height from the magnet to reduce its power. But the result was not satisfactory because after removing it from the oven, the zPDMS didn't conduct electrical current to the components of the circuit.

In conclusion the magnet was too strong for the components (resistors and capacitors) and too weak to align the zPDMS columns.

Despite all, excellent design results were achieved step by step for the completion of the final circuit like:

- Functional ECG circuit with rigid board;
- Functional ECG electrodes with AgPDMS;
- ECG waves and cardiac frequency results;
- Single layer and multi-layer circuits with AgPDMS;
- Creation of vias;
- Integration of chips, resistors and capacitors with zPDMS;
- zPDMS interfacing with the AgPDMS based circuit.

But despite all these advances and different challenges that have been addressed within this thesis, the final circuit was not functional due to unforeseen problems and lack of time, for further implementation of the next versions of the circuit.

Solutions and better implementations on these problems will be discussed and analyzed in the next chapter.

Chapter 6

GENERAL CONCLUSION

In this thesis, new extensible electrodes were analyzed and compared for possible applications in wearable bio-computing with their interfacing with flexible electronics and acquisition systems. Furthermore, different types of connection between components, capacitor chips and resistors, and the flexible circuit have been studied and analyzed.

A new electrode material is hardly going to replace Ag/AgCl electrodes in clinical environment in the near future, as these have exceptional signal quality and are very easy to keep attached to specific positions of a patient's body, besides being relatively cheap and disposable. As for other kinds of applications, the future of biomonitoring might easily reside in PDMS-based electrodes as the ones described in this work (AgPDMS and zPDMS/eGaIn). The usage of comfortable user-friendly materials, like PDMS, that avoid complications such as skin irritation and complex skin preparation are desired. Moreover, PDMS based electrodes have the advantage of conforming better to the subject's skin than currently available rigid dry electrodes, avoiding motion artifacts and skin pressure marks.

The discussion on the quality and usability of flexible circuits in the future is different. They can be used on many aspects of electronic bio-monitoring because they avoid complications in contact with the skin, easily manageable, usable and especially very comfortable; the only problem is their production. In fact, automatic machines should be implemented for two simple reasons: avoid errors due to man's maneuvering (especially for very small circuits) and speed up production; this can

be reduced the errors. It was very difficult to have a two-layer circuit working because the margin of error for each step of production was very small and, as already mentioned, each attempt required about three or four hours to complete.

Regarding the implementation of the components on the circuit, it must be noted that an excellent method for fixing resistors and capacitors was found, but not for the chips, in fact initially with the method shown (4.21) they were easy to implement and very reliable for deformability and stretchability, then, given the need, with the method in figure (5.10) the final circuit has lost some of its initial properties.

6.1 Future Work

The prototype of the circuit in figure (5.11) can be optimized for the implementation of the chips. As discussed in the previous section, the modification on the assembly of the chips has lost at the circuit its deformability and stretchability, so the next step could be to replace the flexible PCB with a flexible double layer PCB (6.1). This will allow a different design and therefore a different fixing of the PCB: imposing the connection on the opposite side of the chips will not have the problem of the space between the circular pads of the circuit and those of the PCB. Moreover this will allow to recover the advantages previously lost.

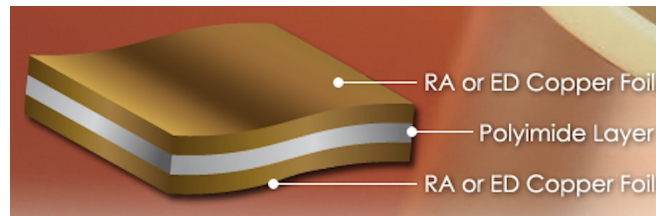


Figure 6.1: Flexible double layer PCB.

Another important element that could be added to the project could be two LEDs: the first one an operating indicator (fixed LED), the second one synchronized with the cardiac frequency (flashing LED).

Finally, the last most important aspect is surely the replacement of the magnet with one of the same dimensions but with a reduced thickness, to avoid the drawbacks discussed in the previous chapter.

We can conclude saying that, through this last substitution and the introduction of

double layer PCBs, the final circuit could guarantee the pre-established result.

Appendix A

Programming code Arduino

```
#include <SPI.h>
#include <TimerOne.h>

#define MAX30003_CS_PIN 7
#define CLK_PIN 6

#ifndef MAX30003_H_
#define MAX30003_H_

#include <arduino.h>

#define WREG 0x00
#define RREG 0x01

#define NO_OP 0x00
#define STATUS 0x01
#define EN_INT 0x02
#define EN_INT2 0x03
#define MNGR_INT 0x04
#define MNGR_DYN 0x05
```

```
#define SW_RST          0x08
#define SYNCH           0x09
#define FIFO_RST        0x0A
#define INFO            0x0F
#define CNFG_GEN        0x10
#define CNFG_CAL        0x12
#define CNFG_EMUX       0x14
#define CNFG_ECG        0x15
#define CNFG_RTOR1     0x1D
#define CNFG_RTOR2     0x1E
#define ECG_FIFO_BURST 0x20
#define ECG_FIFO        0x21
#define RTOR            0x25
#define NO_OP           0x7F
```

```
#endif
```

```
volatile char SPI_RX_Buff[5] ;
volatile char *SPI_RX_Buff_Ptr;
int i=0;
unsigned long uintECGraw = 0;
signed long intECGraw=0;
uint8_t DataPacketHeader[20];
uint8_t data_len = 8;
signed long ecgdata;
unsigned long data;
```

```
char SPI_temp_32b[4];
char SPI_temp_Burst[100];
```

```
// 32KHz clock using timer1
void timerIsr()
{
```

```
digitalWrite( CLK_PIN, digitalRead(CLK_PIN ) ^ 1 );
// toggle Digital6 attached to

}

void setup()
{
  Serial.begin(115200); //Serial begin

  pinMode(MAX30003_CS_PIN,OUTPUT);
  digitalWrite(MAX30003_CS_PIN,HIGH); //disable device

  SPI.begin ();
  SPI.setBitOrder(MSBFIRST);
  SPI.setDataMode(SPI_MODE0);
  SPI.setClockDivider (SPI_CLOCK_DIV4);

  pinMode(CLK_PIN,OUTPUT);

  MAX30003.begin (); // initialize MAX30003

}

void loop()
{
  MAX30003_Reg_Read(ECG_FIFO);

  unsigned long data0 = (unsigned long) (SPI_temp_32b [0]);
  data0 = data0 <<24;
  unsigned long data1 = (unsigned long) (SPI_temp_32b [1]);
  data1 = data1 <<16;
  unsigned long data2 = (unsigned long) (SPI_temp_32b [2]);
  data2 = data2 >>6;
```

```
data2 = data2 & 0x03;

data = (unsigned long) (data0 | data1 | data2);
ecgdata = (signed long) (data);

MAX30003_Reg_Read(RTOR);
unsigned long RTOR_msb = (unsigned long) (SPI_temp_32b[0]);
// RTOR_msb = RTOR_msb <<8;
unsigned char RTOR_lsb = (unsigned char) (SPI_temp_32b[1]);

unsigned long rtor = (RTOR_msb<<8 | RTOR_lsb);
rtor = ((rtor >>2) & 0x3fff) ;

float hr = 60 /((float)rtor*0.008);
unsigned int HR = (unsigned int)hr; // type cast to int

unsigned int RR = (unsigned int)rtor*8 ; //8ms

Serial.print(",");
/* Serial.print(RTOR_lsb);
Serial.print(",");
Serial.print(rtor);
Serial.print(",");
Serial.print(RR);
Serial.print(",");
Serial.println(hr);/*
Serial.print(RR);
DataPacketHeader[0] = 0x0A;
DataPacketHeader[1] = 0xFA;
DataPacketHeader[2] = 0x0C;
DataPacketHeader[3] = 0;
DataPacketHeader[4] = 0x02;
```

```
DataPacketHeader [5] = ecgdata ;
DataPacketHeader [6] = ecgdata >>8;
DataPacketHeader [7] = ecgdata >>16;
DataPacketHeader [8] = ecgdata >>24;

DataPacketHeader [9] = RR ;
DataPacketHeader [10] = RR >>8;
DataPacketHeader [11] = 0x00;
DataPacketHeader [12] = 0x00;

DataPacketHeader [13] = HR ;
DataPacketHeader [14] = HR >>8;
DataPacketHeader [15] = 0x00;
DataPacketHeader [16] = 0x00;

DataPacketHeader [17] = 0x00;
DataPacketHeader [18] = 0x0b;

for (i=0; i<19; i++) // transmit the data
{
    Serial.write(DataPacketHeader [i]);

}

    MAX30003_Reg_Read(INFO);
    unsigned long info = (unsigned long) (SPI_temp_32b [0]);
    Serial.println (info);

delay (1);
}

void MAX30003_Reg_Write (unsigned char WRITE_ADDRESS,
unsigned long data)
```

```
{

// now combine the register address and the command into one byte:
byte dataToSend = (WRITE_ADDRESS<<1) | WREG;

// take the chip select low to select the device:
digitalWrite(MAX30003_CS_PIN, LOW);

delay(2);
SPI.transfer(dataToSend); //Send register location
SPI.transfer(data>>16); //number of register to wr
SPI.transfer(data>>8); //number of register to wr
SPI.transfer(data); //Send value to record into register
delay(2);

// take the chip select high to de-select:
digitalWrite(MAX30003_CS_PIN, HIGH);
}

void max30003_sw_reset(void)
{
MAX30003_Reg_Write(SW_RST,0x000000);
delay(100);
}

void max30003_synch(void)
{
MAX30003_Reg_Write(SYNCH,0x000000);
}

void MAX30003_Reg_Read(uint8_t Reg_address)
{
uint8_t SPI_TX_Buff;
```

```
digitalWrite(MAX30003_CS_PIN, LOW);

SPI_TX_Buff = (Reg.address<<1 ) | RREG;
SPI.transfer(SPI_TX_Buff); //Send register location

for ( i = 0; i < 3; i++)
{
    SPI_temp_32b[i] = SPI.transfer(0xff);
}

digitalWrite(MAX30003_CS_PIN, HIGH);
}

void MAX30003_Read_Data(int num_samples)
{
    uint8_t SPI_TX_Buff;

    digitalWrite(MAX30003_CS_PIN, LOW);

    SPI_TX_Buff = (ECG_FIFO_BURST<<1 ) | RREG;
    SPI.transfer(SPI_TX_Buff); //Send register location

    for ( i = 0; i < num_samples*3; ++i)
    {
        SPI_temp_Burst[i] = SPI.transfer(0x00);
    }

    digitalWrite(MAX30003_CS_PIN, HIGH);
}

void MAX30003_begin()
{
```

```
//Start CLK timer
Timer1.initialize(16); // set a timer of length 100000
        microseconds (or 0.1 sec – or 10Hz => the led will
        blink 5 times, cycles of on–and–off, per second)
Timer1.attachInterrupt(timerIsr); // attach the service routine
        here

max30003_sw_reset ();
delay (100);
MAX30003_Reg_Write(CNFG_GEN, 0x081007);
delay (100);
MAX30003_Reg_Write(CNFG_CAL, 0x720000); // 0x700000
delay (100);
MAX30003_Reg_Write(CNFG_EMUX,0x0B0000);
delay (100);
MAX30003_Reg_Write(CNFG_ECG, 0x005000); // d23 – d22 : 10
        for 250sps , 00:500sps

delay (100);

MAX30003_Reg_Write(CNFG_RTOR1,0x3fc600);
max30003_synch ();
delay (100);
}
```

Appendix B

Programming PSoC creator

```
#include "app_UART.h"  
#include "app_Ble.h"
```

```
#define WREG 0x00  
#define RREG 0x01
```

```
#define NO_OP          0x00  
#define STATUS        0x01  
#define EN_INT        0x02  
#define EN_INT2       0x03  
#define MNGR_INT      0x04  
#define MNGR_DYN      0x05  
#define SW_RST        0x08  
#define SYNCH         0x09  
#define FIFO_RST      0x0A  
#define INFO          0x0F  
#define CNFG_GEN      0x10  
#define CNFG_CAL      0x12  
#define CNFG_EMUX     0x14  
#define CNFG_ECG      0x15  
#define CNFG_RTOR1    0x1D
```

```
#define CNFG_RTOR2      0x1E
#define ECG_FIFO_BURST 0x20
#define ECG_FIFO       0x21
#define RTOR           0x25
#define NO.OP         0x7F

volatile char SPI_RX_Buff[5] ;
volatile char *SPI_RX_Buff_Ptr;
int i=0;
unsigned long uintECGraw = 0;
signed long intECGraw=0;
uint8_t DataPacketHeader[20];
uint8_t data_len = 8;
signed long ecgdata;

char SPI_temp_32b[4];
char SPI_temp_Burst[100];

#define SPLWAIT_TXDONE()
while(0u==(SPI_GetMasterInterruptSource() &
           SPLINTR_MASTER_SPLDONE)){}
SPI_ClearMasterInterruptSource(SPLINTR_MASTER_SPLDONE);

void MAX30003_Reg_Write
(unsigned char WRITE_ADDRESS, unsigned long data)
{
    uint8 dataToSend = (WRITE_ADDRESS<<1) | WREG;

    // take the chip select low to select the device:
    CS_Write(0);
    CyDelay(2);
    SPI_SpiUartWriteTxData(dataToSend); //Send register location
    SPLWAIT_TXDONE();
}
```

```
SPI_SpiUartWriteTxData(data >>16); //number of register to wr
    SPLWAIT_TXDONE();
SPI_SpiUartWriteTxData(data >>8); //number of register to wr
    SPLWAIT_TXDONE();
SPI_SpiUartWriteTxData(data); //Send value to record into register
    SPLWAIT_TXDONE();
CyDelay(2);

// take the chip select high to de-select //
CS_Write(1);
}

void max30003_sw_reset(void)
{
    MAX30003_Reg_Write(SW_RST,0x000000);
    CyDelay(100);
}

void max30003_synch(void)
{
    MAX30003_Reg_Write(SYNCH,0x000000);
}

void MAX30003_Reg_Read(uint8_t Reg_address)
{
    uint8_t SPI_TX_Buff;
    CS_Write(0);
    CyDelayUs(1);
    SPI_SpiUartClearTxBuffer();
    SPI_TX_Buff = (Reg_address <<1) | RREG;
    SPI_SpiUartWriteTxData(SPI_TX_Buff); //Send register location
    SPLWAIT_TXDONE();
    SPI_SpiUartClearRxBuffer();
}
```

```
for ( i = 0; i < 3; i++)
{
    SPI_SpiUartWriteTxData(0);
    SPIWAIT_TXDONE();
    while(0u != SPI_SpiIsBusBusy());
    SPI_temp_32b[i] = SPI_SpiUartReadRxData();
}
CyDelayUs(1);
CS_Write(1);
}

void MAX30003_begin()
{
    max30003_sw_reset();
    CyDelay(100);
    MAX30003_Reg_Write(CNFG_GEN, 0x081007);
    CyDelay(100);
    MAX30003_Reg_Write(CNFG_CAL, 0x720000); // 0x700000
    CyDelay(100);
    MAX30003_Reg_Write(CNFG_EMUX, 0x0B0000);
    CyDelay(100);
    MAX30003_Reg_Write(CNFG_ECG, 0x005000); // d23 – d22 : 10 for
                                                250sps , 00:500 sps
    CyDelay(100);
    MAX30003_Reg_Write(CNFG_RTOR1, 0x3fc600);
    max30003_synch();
    CyDelay(100);
}

void HandleBLE_Data(uint16 txDataClientConfigDesc)
{
    uint8    uartTxData[mtuSize - 3];
```

```
uint16  uartTxDataLength;
CYBLE_API_RESULT_T          bleApiResult;
CYBLE_GATTS_HANDLE_VALUE_NTF_T  uartTxDataNtf;
uint8  k;
uint16  value;

MAX30003_Reg_Read(ECG_FIFO);
unsigned long data;
unsigned long data0 = (unsigned long) (SPI_temp_32b[0]);
data0 = data0 <<24;
unsigned long data1 = (unsigned long) (SPI_temp_32b[1]);
data1 = data1 <<16;
unsigned long data2 = (unsigned long) (SPI_temp_32b[2]);
data2 = data2 >>6;
data2 = data2 & 0x03;
data = (unsigned long) (data0 | data1 | data2);
ecgdata = (signed long) (data);

MAX30003_Reg_Read(RTOR);
unsigned long RTOR_msb = (unsigned long) (SPI_temp_32b[0]);
// RTOR_msb = RTOR_msb <<8;
unsigned char RTOR_lsb = (unsigned char) (SPI_temp_32b[1]);
unsigned long rtor = (RTOR_msb<<8 | RTOR_lsb);
rtor = ((rtor >>2) & 0x3fff) ;

float hr = 60 /((float)rtor*0.008);
unsigned int HR = (unsigned int)hr; // type cast to int
unsigned int RR = (unsigned int)rtor*8 ; //8ms

DataPacketHeader[0] = 0x0A;
DataPacketHeader[1] = 0xFA;
DataPacketHeader[2] = 0x0C;
DataPacketHeader[3] = 0;
```

```
DataPacketHeader [4] = 0x02;

DataPacketHeader [5] = ecgdata;
DataPacketHeader [6] = ecgdata >>8;
DataPacketHeader [7] = ecgdata >>16;
DataPacketHeader [8] = ecgdata >>24;

DataPacketHeader [9] = RR ;
DataPacketHeader [10] = RR >>8;
DataPacketHeader [11] = 0x00;
DataPacketHeader [12] = 0x00;

DataPacketHeader [13] = HR ;
DataPacketHeader [14] = HR >>8;
DataPacketHeader [15] = 0x00;
DataPacketHeader [16] = 0x00;

DataPacketHeader [17] = 0x00;
DataPacketHeader [18] = 0x0b;

for (i=0; i<19; i++) // transmit the data
{
    uartTxData [ i ] = DataPacketHeader [ i ];
}

uartTxDataLength = 19;

if ((0 != uartTxDataLength) &&
    (NOTIFICATION_ENABLED == txDataClientConfigDesc))
{
    uartTxDataNtf.value.val = uartTxData;
    uartTxDataNtf.value.len = uartTxDataLength;
    uartTxDataNtf.attrHandle = CYBLE_SERVER_UART_SERVER
```

```

_UART_TX_DATA_CHAR_HANDLE;

do
{
    bleApiResult = CyBle_GattsNotification
                  (cyBle_connHandle , &uartTxDataNtf);
    CyBle_ProcessEvents ();
}
while ((CYBLE_ERROR_OK != bleApiResult) &&
       (CYBLE_STATE_CONNECTED == cyBle_state));
}
}

void HandleUartTxTraffic(uint16 txDataClientConfigDesc)
{
    uint8    index;
    uint8    uartTxData[mtuSize - 3];
    uint16   uartTxDataLength;

    static uint16 uartIdleCount = UART_IDLE_TIMEOUT;

    CYBLE_APLRESULT_T          bleApiResult;
    CYBLE_GATTS_HANDLE_VALUE_NTF_T  uartTxDataNtf;

    uartTxDataLength = UART_SpiUartGetRxBufferSize ();

#ifdef FLOW_CONTROL
    if (uartTxDataLength >= (UART_UART_RX_BUFFER_SIZE -
                             (UART_UART_RX_BUFFER_SIZE/2)))
    {
        DisableUartRxInt ();
    }
    else

```

```
    {
        EnableUartRxInt ();
    }
#endif

if((0 != uartTxDataLength) &&
    (NOTIFICATIONENABLED == txDataClientConfigDesc))
{
    if(uartTxDataLength >= (mtuSize - 3))
    {
        uartIdleCount      = UART_IDLE_TIMEOUT;
        uartTxDataLength   = mtuSize - 3;
    }
    else
    {
        if(--uartIdleCount == 0)
        {
            /*uartTxDataLength remains unchanged */;
        }
        else
        {
            uartTxDataLength = 0;
        }
    }
}

if(0 != uartTxDataLength)
{
    uartIdleCount      = UART_IDLE_TIMEOUT;

    for(index = 0; index < uartTxDataLength; index++)
    {
        uartTxData[index] = (uint8) UART_UartGetByte();
    }
}
```

```
    uartTxDataNtf.value.val = uartTxData;
    uartTxDataNtf.value.len = uartTxDataLength;
    uartTxDataNtf.attrHandle = CYBLE_SERVER_UART_SERVER
                               _UART_TX_DATA_CHAR_HANDLE;

#ifdef FLOWCONTROL
    DisableUartRxInt();
#endif

do
{
    bleApiResult = CyBle_GattsNotification
                  (cyBle_connHandle, &uartTxDataNtf);
    CyBle_ProcessEvents();
}
while((CYBLE_ERROR_OK != bleApiResult) &&
      (CYBLE_STATE_CONNECTED == cyBle_state));
}
}

void HandleUartRxTraffic(CYBLE_GATTS_WRITE_REQ_PARAM_T*uartRxDataWrReq)
{
    if(uartRxDataWrReq->handleValPair.attrHandle ==
        CYBLE_SERVER_UART_SERVER_UART_RX_DATA_CHAR_HANDLE)
    {
        UART_SpiUartPutArray(uartRxDataWrReq->handleValPair.value.val, \
            (uint32) uartRxDataWrReq->handleValPair.value.len);
    }
}

void DisableUartRxInt(void)
```

```
{  
    UART_INTR_RX_MASK_REG &= ~UART_RX_INTR_MASK;  
}
```

```
void EnableUartRxInt(void)  
{  
    UART_INTR_RX_MASK_REG |= UART_RX_INTR_MASK;  
}
```

Bibliography

- [1] <http://afra-tech.com/en/products/microfluidics-pdms-station-soft-lithography>.
- [2] <http://anesthetistway.com/page/2>.
- [3] <https://www.github.com/Protocentral/protocentralmax30003>.
- [4] <https://www.intertronics.co.uk/product/thinky-are-250-mixing-degassing-planetary-mixer/>.
- [5] <https://www.mddionline.com/what-are-wearables-good-research-partnership-wants-find-out>.
- [6] <https://www.printedelectronicsworld.com/articles/13049/hybrid-3-d-printing-method-for-flexible-electronics>.
- [7] <https://www.ulsinc.com/learn/laser-cutting>.
- [8] <http://transene.com/silver-epoxy/>.
- [9] <http://www.zehntner.com/products/categories/application/zua-2000>.
- [10] Nicholas A Peppas. *The Biomedical Engineering Handbook, second edition, two volumes: J.D. Bronzino, editor, CRC Press and IEEE Press, Boca Raton, FL, 2000, 189.95, 3024pp., volume 71.042001*.
- [11] John A. Rogers, Roozbeh Ghaffari, and Dae-Hyeong Kim. *Stretchable Bioelectronics for Medical Devices and Systems*. 01 2016.

- [12] Emanuele Cattarinuzzi. *Meccanica dei dispositivi di stretchable electronics : caratterizzazione dei materiali costituenti e comportamento meccanico delle interconnessioni*, 2012.
- [13] Yu M. Chi, Patrick Ng, Eric Kang, Joseph Kang, Jennifer Fang, and Gert Cauwenberghs. Wireless non-contact cardiac and neural monitoring. In *Wireless Health 2010*, WH '10, pages 15–23, New York, NY, USA, 2010. ACM.
- [14] Rex Ching. Realtime ecg monitoring with deep learning, September 2017.
- [15] Nicholas Cram. Book review: Medical instrumentation, application & design, 3rd ed., by john g. webster. *Annals of Biomedical Engineering*, 28(2):218–218, Feb 2000.
- [16] Scott Day. Important factors in surface emg measurement. pages 1–17, 01 2002.
- [17] Michael D. Dickey, Ryan C. Chiechi, Ryan J. Larsen, Emily A. Weiss, David A. Weitz, and George M. Whitesides. Eutectic gallium-indium (egain): A liquid metal alloy for the formation of stable structures in microchannels at room temperature. *Advanced Functional Materials*, 18(7):1097–1104, 2008.
- [18] Daniel E Becker. Fundamentals of electrocardiography interpretation. 53:53–63; quiz 64, 02 2006.
- [19] Andrew Fassler and Carmel Majidi. 3d structures of liquid-phase gain alloy embedded in pdms with freeze casting. *Lab Chip*, 13:4442–4450, 2013.
- [20] Reza Ghodssi and Pinyen Lin. *Mems materials and processes handbook*. Springer, 2011.
- [21] Davide Vaz Gomes. Stretchable skin for biomonitoring. page 104, 2017.
- [22] Michael R. Neuman John G. Webster. *Medical instrumentation application and design*, 4th edition.
- [23] Gary Kamen and 1961-(viaf)103384635 Gabriel, David A. *Essentials of electromyography*. Leeds : Human Kinetics, 2010.

- [24] Stephen Lee and John Kruse. Biopotential electrode sensors in ecg/eeg/emg systems. 01 2008.
- [25] Tong Lu, Lauren Finkenauer, James Wissman, and Carmel Majidi. Rapid prototyping for soft-matter electronics. *Advanced Functional Materials*, 24(22):3351–3356, 2014.
- [26] Tong Lu, James Wissman, Ruthika, and Carmel Majidi. Soft anisotropic conductors as electric vias for ga-based liquid metal circuits. *ACS Applied Materials & Interfaces*, 7(48):26923–26929, 2015. PMID: 26569575.
- [27] D. Spelmezan, A. Schanowski, and J. Borchers. Rapid prototyping for wearable computing. In *2008 12th IEEE International Symposium on Wearable Computers*, pages 109–110, 2008.
- [28] Yuan Wei, Zhensong Xu, Mark A Cachia, John Nguyen, Yi Zheng, Chen Wang, and Yu Sun. Embedded silver pdms electrodes for single cell electrical impedance spectroscopy. *Journal of Micromechanics and Microengineering*, 26(9):095006, 2016.
- [29] Refet Firat Yazicioglu, Chris Van Hoof, and Robert Puers. *Biopotential Read-out Circuits for Portable Acquisition Systems*. Springer Publishing Company, Incorporated, 1st edition, 2008.
- [30] Wei Zhang, Abbas A. Dehghani-Sani, and Richard S. Blackburn. Carbon based conductive polymer composites. *Journal of Materials Science*, 42(10):3408–3418, May 2007.

Acknowledgements

Desidero ricordare tutti coloro che mi hanno aiutato nella stesura della tesi con suggerimenti, critiche ed osservazioni: a loro va la mia gratitudine, anche se a me spetta la responsabilità per ogni errore contenuto in questa tesi.

Ringrazio anzitutto il professor Chiaberge Marcello ed il professor Mahmoud Tavakoli: senza il loro supporto e la loro guida sapiente questa tesi non esisterebbe. Proseguo con Pedro Lopes e Luìs Negrão per il loro infinito aiuto durante questo periodo.

Un ringraziamento particolare va alla mia famiglia senza alcun dubbio primo punto fisso della mia vita, così come lo sono gli amici d'infanzia che, anche se distanti, sono sempre persone su cui posso contare.

Parole a parte vanno spese per il mio #teampizza: le persone vanno e vengono ma alcune, le più preziose, rimarranno. Grazie di tutto!

Ringrazio infine anche i colleghi di università, anche loro sempre presenti per consigli e supporto.